Embedded Firmware Solutions for Intelligent IoT Applications

Dr. A. VIJAYALAKSHMI
Mrs. DIMPLE JUNEJA
Dr. A. DHANASEKARAN
Dr. P. BRINDHA DEVI

SRR
Publicizing Research

ISBN 978-816860177-2

Embedded Firmware Solutions for Intelligent IoT Applications

April 2026

Dr. A. VIJAYALAKSHMI
Professor and HoD
Department of Electronics and Communication Engineering
Vels Institute of Science, Technology & Advanced Studies
Chennai, Tamil Nadu, India.

Mrs. DIMPLE JUNEJA
Research Scholar, Department of Education
Mohanlal Sukhadia University
Udaipur, Rajasthan, India.

Dr. A. DHANASEKARAN
Associate Professor, Department of Mechanical Engineering
Academy of Maritime Education and Training (AMET)
Deemed to be University, Chennai, Tamil Nadu, India.

Dr. P. BRINDHA DEVI
Associate Professor, Department of Bioengineering
Vels Institute of Science Technology & Advanced Studies
Chennai, Tamil Nadu, India.

April 2026

ISBN: 978-81-686017-7-2

Published By

SRR
Publicizing Research

SCIENTIFIC RESEARCH REPORTS
(A Book Publisher, approved by Govt. of India)

I Floor, S S Nagar, Chennai - 600 087,
Tamil Nadu, India.

editors@srrbooks.in, contact@srrbooks.in
www.srrbooks.in

PREFACE

The rapid evolution of the Internet of Things (IoT) has fundamentally transformed the way devices interact, communicate, and operate within modern digital ecosystems. At the heart of this transformation lies embedded firmware an essential layer that bridges hardware capabilities with intelligent software behavior. As IoT systems continue to expand across domains such as smart homes, industrial automation, healthcare, agriculture, and transportation, the demand for efficient, reliable, and scalable firmware solutions has become increasingly critical.

This book, *Embedded Firmware Solutions for Intelligent IoT Applications*, is conceived to provide a comprehensive and structured understanding of firmware design principles tailored specifically for IoT environments. It addresses the growing need for engineers, researchers, and students to grasp both foundational concepts and advanced techniques required to develop robust embedded systems capable of operating under constraints such as limited power, memory, and processing resources.

The content is systematically organized to guide the reader from core fundamentals to advanced implementation strategies. It begins with an exploration of embedded firmware design principles, development environments, and system architectures, establishing a strong conceptual base. Building upon this, the book delves into microcontroller architectures and peripheral integration, offering practical insights into hardware interfacing and resource management.

A significant portion of the book is dedicated to real-time operating systems (RTOS) and task scheduling, which are crucial for managing concurrent operations in time-sensitive IoT applications. The discussion then extends to communication protocols and connectivity management, covering both wired and wireless technologies that enable seamless device interaction within distributed networks.

Security and reliability are emphasized as essential components of modern firmware design. The book examines strategies for safeguarding IoT devices against vulnerabilities while ensuring system stability and fault tolerance. Additionally, power optimization techniques are explored to address the energy constraints inherent in many embedded systems, particularly those operating in remote or battery-powered environments.

Recognizing the growing importance of intelligent systems, the final sections introduce edge intelligence and AI-enabled firmware solutions. These chapters highlight how machine learning and data-driven approaches can be integrated into embedded platforms to enable real-time decision-making and enhanced system autonomy.

This book is intended to serve as both an academic reference and a practical guide. It is suitable for undergraduate and postgraduate students in electronics, computer science, and related disciplines, as well as professionals engaged in embedded system design and IoT development. By combining theoretical foundations with application-oriented perspectives, it aims to equip readers with the knowledge and skills necessary to design next-generation embedded firmware solutions that are efficient, secure, and

intelligent. It is our hope that this work will contribute meaningfully to the advancement of embedded systems engineering and inspire further innovation in the dynamic field of IoT.

We extend our sincere thanks to our publisher, Scientific Research Reports, Chennai, India, for their dedicated efforts in preparing this book and for ensuring the inclusion of enriched and high-quality technical content.

Wishes and Regards,

Dr. A. VIJAYALAKSHMI
Professor and HoD
Department of Electronics and Communication Engineering
Vels Institute of Science, Technology & Advanced Studies
Chennai, Tamil Nadu, India.

Mrs. DIMPLE JUNEJA
Research Scholar, Department of Education
Mohanlal Sukhadia University
Udaipur, Rajasthan, India.

Dr. A. DHANASEKARAN
Associate Professor, Department of Mechanical Engineering
Academy of Maritime Education and Training (AMET)
Deemed to be University, Chennai, Tamil Nadu, India.

Dr. P. BRINDHA DEVI
Associate Professor, Department of Bioengineering
Vels Institute of Science Technology & Advanced Studies
Chennai, Tamil Nadu, India.

CONTENTS


SRR
Publicizing Research

Section 1

Fundamentals of Embedded Firmware Design for IoT Systems

1.1 Introduction

The proliferation of connected devices across industrial, consumer, and infrastructure domains has positioned embedded firmware as the foundational intelligence layer of the Internet of Things (IoT) ecosystem. Firmware, defined as the low-level software permanently programmed into a device's non-volatile memory, governs the direct interaction between hardware peripherals and higher-level application logic. Unlike conventional software operating on general-purpose processors, embedded firmware must operate within severe constraints of memory footprint, computational throughput, power budget, and real-time determinism (Barr & Massa, 2006). Understanding these constraints is not merely academic; it determines the commercial viability, field reliability, and security posture of every IoT deployment.

In IoT environments, firmware serves as the critical enabler of device intelligence—translating raw sensor signals into meaningful data, executing control algorithms, managing communication protocols, and maintaining operational continuity in the absence of human intervention. A temperature sensor node in an industrial monitoring system, for instance, relies entirely on its firmware to perform analog-to-digital conversion, apply calibration coefficients, package data into MQTT payloads, and transmit over a LoRaWAN link while sustaining operation on a coin-cell battery for years (Hahm et al., 2016). This multiplicity of responsibilities, performed simultaneously on microcontrollers with as little as 2 KB of RAM, underscores the

ISBN 978-816860177-2

engineering sophistication demanded of embedded firmware developers.

The design of robust IoT firmware must simultaneously address determinism, portability, maintainability, and security. Determinism ensures that time-critical interrupt service routines execute within guaranteed latency bounds, which is essential in process control and medical monitoring applications. Portability enables firmware modules to migrate across hardware revisions without wholesale rewrites, dramatically reducing development costs. Maintainability, achieved through structured layering and modular design, supports firmware updates over the device lifecycle, which may span a decade or more in industrial deployments (Kuon et al., 2008). Security considerations, including secure boot, encrypted firmware images, and authenticated over-the-air (OTA) updates, have become non-negotiable as IoT attack surfaces expand exponentially.

This section establishes the conceptual and technical foundation upon which subsequent sections build. It introduces the layered architecture model governing modern embedded firmware, examines the development lifecycle and associated toolchains, and addresses the memory management strategies that allow capable software to operate within the stringent resource envelopes of IoT microcontrollers. Collectively, these fundamentals equip engineers and researchers with the structured framework necessary to design firmware that is not merely functional, but intelligent, resilient, and production-ready across the full diversity of IoT application domains.

1.2 Embedded System Architecture and Firmware Layers

Embedded system architecture for IoT applications is governed by the principle of **hardware–software co-design**, wherein hardware

capabilities and firmware requirements are defined concurrently rather than sequentially. This co-design philosophy ensures that peripheral configurations, interrupt priorities, clock domains, and power management states are reflected in the firmware architecture from the earliest design phase, minimizing integration risk and optimizing system-level performance (Wolf, 2012). The result is a layered firmware stack in which each layer presents a well-defined abstraction interface to the layer above, enabling independent development, testing, and replacement of individual components.

1.2.1 Layered Firmware Architecture

The canonical firmware stack in IoT embedded systems comprises four primary layers: the **bootloader**, the Hardware Abstraction Layer (HAL), device drivers and middleware, and the application layer. The bootloader executes immediately upon power-on reset, performing hardware initialization, memory integrity verification, and conditional invocation of firmware update procedures before transferring control to the main application image. Modern secure bootloaders implement cryptographic signature verification using SHA-256 hashing and RSA-2048 or ECDSA-256 digital signatures, ensuring that only authenticated firmware images execute on the device (ARM Limited, 2019).

The Hardware Abstraction Layer sits immediately above the bootloader, providing a standardized API for accessing microcontroller peripherals—GPIOs, timers, UART, SPI, I²C, ADC—independent of the specific silicon vendor or chip revision. Industry-standard HAL implementations, such as STMicroelectronics' STM32 HAL or Nordic Semiconductor's nRF5 SDK, reduce peripheral access code to vendor-neutral function calls. Above the HAL reside

ISBN 978-816860177-2

middleware components including real-time operating system (RTOS) kernels, communication stacks (TCP/IP, BLE, Zigbee, LoRaWAN), file systems, and sensor fusion libraries. The application layer, occupying the topmost position, implements device-specific business logic, data processing pipelines, and cloud connectivity protocols.

Key architectural principles that govern effective IoT firmware layering include:

- **Abstraction Boundaries:** Each layer must expose only the minimum necessary interface to the layer above, preventing cross-layer dependencies that impair portability and testability across hardware platforms.
- **Interrupt Isolation:** Interrupt Service Routines (ISRs) must execute in the shortest possible time—typically under 10 µs—deferring complex processing to task or thread contexts to preserve system determinism.
- Dependency injection and callback mechanisms at middleware interfaces ensure that application code remains **decoupled from protocol-specific implementations**, facilitating protocol stack substitution without application rewrites.

1.2.2 Hardware–Software Interface and Portability

Portability across hardware platforms is a strategic imperative in commercial IoT product development, where a single firmware codebase may need to support multiple microcontroller families across product generations. Achieving portability requires rigorous adherence to the **Board Support Package (BSP)** pattern, wherein all hardware-specific configurations—pin mappings, clock frequencies, peripheral assignments—are isolated within a dedicated BSP module, leaving all other firmware layers hardware-agnostic (Massa, 2003).

The impact of disciplined layering on development efficiency is quantifiable: studies of commercial embedded software projects report that well-abstracted firmware architectures reduce porting effort by **40–60%** when migrating to a new hardware platform, compared to monolithic firmware designs (Barr & Massa, 2006). Furthermore, layered architectures support unit testing of individual firmware modules in host-machine environments using frameworks such as Unity or CppUTest, enabling continuous integration pipelines that catch regressions before hardware deployment.

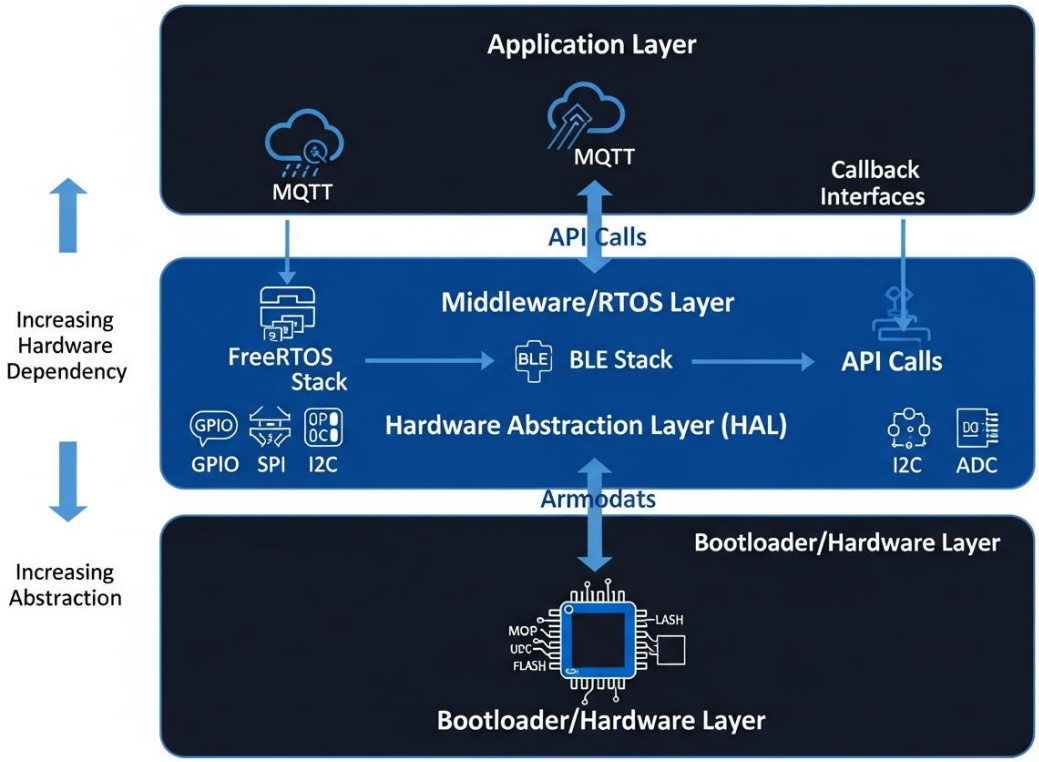

Figure 1.1: Layered firmware architecture for IoT embedded systems showing abstraction hierarchy from hardware to application.

1.3 Firmware Development Lifecycle and Toolchains

The firmware **development lifecycle** in IoT systems extends far beyond initial coding, encompassing requirements analysis,

ISBN 978-816860177-2

architectural design, implementation, static analysis, hardware-in-the-loop testing, field deployment, and long-term maintenance through OTA update mechanisms. Each phase carries distinct toolchain requirements and quality gates, and the maturity of lifecycle management practices directly correlates with product reliability metrics in field deployment (Kuon et al., 2008). A disciplined lifecycle approach is especially critical for IoT devices, which often operate in physically inaccessible locations and must maintain correct behavior for operational periods exceeding five to ten years.

1.3.1 Development Phases and Integrated Development Environments

The firmware development process begins with a requirements capture phase that translates system-level specifications—sampling rates, communication protocols, power budgets, latency targets—into firmware design constraints. This is followed by architectural design, where the layered stack, RTOS task decomposition, memory budgets, and interrupt priority schemes are formally defined. The implementation phase employs Integrated Development Environments (IDEs) such as **Eclipse-based tools** (STM32CubeIDE, MCUXpresso), SEGGER Embedded Studio, or the ARM Keil MDK, which integrate source editors, project management, cross-compilers (GCC-ARM, IAR EWARM), and hardware debuggers into a unified environment.

Compilation toolchains for ARM Cortex-M targets—the dominant architecture in IoT microcontrollers with over **85% market share** in 32-bit embedded applications—generate optimized machine code targeting Thumb-2 instruction sets, achieving code density

improvements of 25–30% over equivalent ARM instruction encoding (ARM Limited, 2019). Linker scripts precisely control the placement of code sections (.text), initialized data (.data), zero-initialized data (.bss), and stack/heap regions within the device's flash and RAM memory map, a process fundamental to memory-constrained firmware operation.

Table 1.1 summarizes the principal development phases, associated tools, and quality metrics applicable to IoT firmware projects across the lifecycle.

Table 1.1: IoT Firmware Development Lifecycle Phases, Tools, and Quality Metrics

Lifecycle Phase	Primary Tools	Quality Gate / Metric	Typical Duration (% of project)
Requirements & Architecture	DOORS, draw.io, ArchiMate	Requirements traceability matrix completeness ≥ 95%	10–15%
Implementation & Compilation	STM32CubeIDE, GCC-ARM, IAR EWARM	Static analysis defect density < 0.5 defects/KLOC	30–40%
Debugging & Hardware Testing	SEGGER J-Link, OpenOCD, JTAG/SWD probes	Code coverage ≥ 80%; ISR latency within spec	20–30%
CI/CD & OTA Deployment	GitHub Actions, Jenkins, AWS IoT Jobs	Build success rate ≥ 99%; OTA rollback < 2%	10–15%

1.3.2 Version Control, CI/CD, and OTA Update Strategies

Modern IoT firmware development mandates rigorous **version control practices** using Git-based workflows, with branch protection policies, mandatory code review gates, and automated build triggers. Continuous Integration pipelines execute static analysis tools—PC-

ISBN 978-816860177-2

lint, Polyspace, Coverity—on every commit, enforcing MISRA-C:2012 compliance rules that reduce runtime error probability in safety-relevant embedded applications. MISRA-C adoption has been empirically linked to a **30–50% reduction** in field defect rates in automotive and industrial embedded systems (MISRA Consortium, 2013).

Over-the-Air (OTA) firmware update capability has transitioned from a convenience feature to a security-critical requirement in IoT deployments. The OTA process involves downloading a new firmware binary to a secondary flash partition, verifying its cryptographic signature, and performing an atomic swap of the active and update partitions upon confirmed integrity. Frameworks such as **MCUboot** (an open-source secure bootloader), AWS IoT Jobs, and Azure IoT Hub Device Update implement this dual-bank update pattern, providing rollback protection that automatically reverts to the previous image if the new firmware fails to boot within a defined watchdog interval.

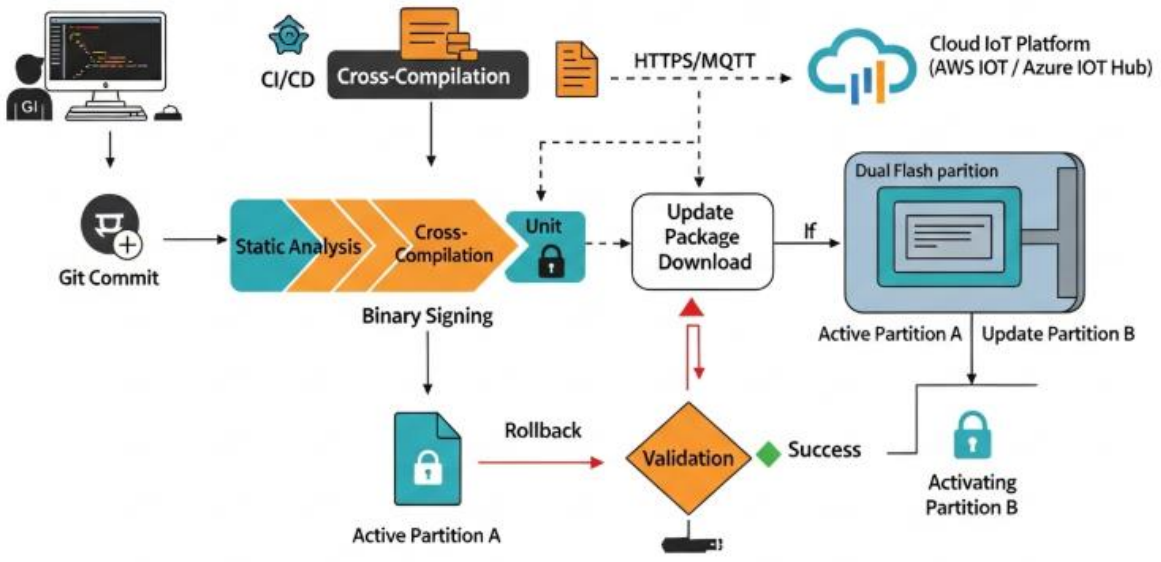

Figure 1.2: CI/CD pipeline and OTA firmware update flow with dual-bank partition management and cryptographic validation.

1.4 Memory Management and Resource Constraints

Memory management represents perhaps the most technically demanding discipline in embedded firmware engineering, as IoT microcontrollers routinely impose aggregate memory budgets that challenge even minimally functional software designs. A typical Cortex-M0+ device such as the STM32L010 provides **8 KB of RAM and 32 KB of flash**, within which the firmware must accommodate the interrupt vector table, bootloader, RTOS kernel, communication stack, application logic, calibration data, and runtime stacks for all concurrent tasks (STMicroelectronics, 2021). Effective memory management therefore requires a comprehensive strategy spanning static allocation, stack sizing, heap discipline, flash storage optimization, and compile-time memory budget enforcement.

1.4.1 Memory Architecture: RAM, Flash, and EEPROM

The memory architecture of IoT microcontrollers is heterogeneous, encompassing distinct storage types with differing access characteristics, write endurance, and power consumption profiles. **Flash memory**, used for firmware code and read-only data, supports 10,000 to 100,000 write cycles and provides non-volatile retention exceeding 10 years at 85°C. RAM provides fast read-write access for runtime variables, stack frames, and dynamically allocated buffers, but is volatile and typically consumes significantly more power per bit than flash in active operation. EEPROM or emulated EEPROM—implemented in flash using wear-leveling algorithms—stores device-specific configuration, calibration coefficients, and operational counters, with typical endurance of 100,000 to 1,000,000 write cycles depending on implementation.

ISBN 978-816860177-2

Table 1.2 presents comparative specifications across memory types commonly deployed in IoT microcontrollers, including capacity ranges, access latency, endurance, and power characteristics relevant to firmware design decisions.

Table 1.2: Memory Type Characteristics in IoT Microcontroller Platforms

Memory Type	Typical Capacity (IoT MCU)	Access Latency	Write Endurance (Cycles)
Internal Flash	16 KB – 2 MB	1–3 wait states at 64 MHz	10,000 – 100,000
SRAM	2 KB – 512 KB	0 wait states (single-cycle)	Unlimited (volatile)
EEPROM (emulated)	512 B – 64 KB	1–5 ms per write operation	100,000 – 1,000,000
External QSPI Flash	1 MB – 256 MB	30–100 ns (memory-mapped)	100,000 (typical NOR)

The allocation of RAM among stack, heap, and static regions requires deliberate engineering judgment. **Static allocation**, in which all variables are declared at compile time with fixed addresses, is the most predictable strategy, eliminating heap fragmentation and stack overflow risks entirely. MISRA-C:2012 guidelines and the CERT C coding standard both recommend eliminating dynamic memory allocation (malloc/free) in safety-critical embedded applications for precisely this reason (MISRA Consortium, 2013). Where dynamic allocation is unavoidable, memory pool allocators—pre-allocating fixed-size blocks at startup—provide bounded allocation time and zero fragmentation, making them suitable for RTOS-based IoT firmware.

Key principles governing memory management in resource-constrained IoT firmware include:

- **Stack Depth Analysis:** Each RTOS task must be assigned a stack sized to accommodate its maximum call depth plus ISR

preemption overhead; tools like SEGGER SystemView and FreeRTOS's uxTaskGetStackHighWaterMark() enable empirical stack usage profiling, with recommended headroom of **25–30%** above measured peak usage.

- **Flash Footprint Optimization:** Compiler optimization flags (-Os for size, link-time optimization), selective inclusion of library functions, and elimination of unused peripheral driver modules can reduce firmware binary size by **15–35%**, preserving flash capacity for application logic and OTA update images.
- **Data Compression and Packing:** Applying bit-field structures, packing pragmas, and run-length encoding to configuration and calibration data stored in flash reduces EEPROM emulation wear and extends the device's operational lifetime in high-write-frequency deployments.

1.4.2 Resource Optimization Strategies and Practical Constraints

Beyond individual memory region management, holistic **resource optimization** in IoT firmware requires coordinated management of CPU cycles, peripheral DMA channels, interrupt priorities, and power states. The relationship between resource consumption and system capability is non-linear: an improperly sized task stack wastes RAM while an undersized stack causes catastrophic overflow; an overly aggressive sleep strategy reduces power consumption but may violate communication protocol timing constraints.

Real-time performance profiling using hardware instrumentation—logic analyzers, oscilloscopes monitoring GPIO toggle markers, or dedicated trace interfaces such as ARM's **Embedded Trace Macrocell (ETM)**—provides cycle-accurate visibility into firmware

ISBN 978-816860177-2

execution timing, enabling targeted optimization of computationally intensive routines. DSP extensions available on Cortex-M4 and Cortex-M33 cores, including single-instruction multiply-accumulate (MAC) operations and SIMD instructions, accelerate signal processing tasks such as FIR filtering and FFT computation by factors of **3–8×** compared to software implementations on non-DSP cores (ARM Limited, 2019).

Memory-mapped I/O through DMA (Direct Memory Access) controllers eliminates CPU involvement in high-throughput peripheral data transfers—ADC sample buffers, SPI display transfers, UART receive queues—freeing processor cycles for application computation. In a representative industrial sensor node, DMA-driven ADC sampling at 100 ksps reduced CPU load from **65% to under 8%**, enabling concurrent execution of communication and data processing tasks that would otherwise have been serialized (Hahm et al., 2016).

Case studies from commercial deployments reinforce the criticality of disciplined resource management: a smart metering platform for 500,000 deployed electricity meters required a firmware refactoring effort to reduce RAM consumption by 22% after field data revealed stack overflows under specific communication load patterns, demonstrating that theoretical analysis must be validated against real-world operational scenarios (Hahm et al., 2016; Wolf, 2012).

1.5 Summary

This section has established the foundational principles of embedded firmware design as applied to IoT systems, spanning architectural organization, development lifecycle management, and the critical discipline of memory and resource management. The layered

firmware architecture—comprising bootloader, HAL, middleware, and application layers—provides the abstraction and modularity necessary for portable, maintainable, and secure IoT firmware across diverse hardware platforms. The firmware development lifecycle, when supported by appropriate IDEs, cross-compilation toolchains, MISRA-compliant static analysis, and CI/CD automation, transforms firmware engineering from an ad hoc practice into a rigorous engineering discipline capable of producing field-reliable software at industrial scale. Memory management, encompassing the disciplined allocation of flash, RAM, and EEPROM resources through static allocation strategies, stack profiling, and DMA utilization, is the mechanism by which capable firmware intelligence is realized within the severe resource constraints that define IoT microcontroller platforms. Together, these fundamentals form the bedrock upon which the specialized topics of subsequent sections—real-time operating systems, connectivity protocol firmware, power management, and security—are constructed.

References

[1] ARM Limited. (2019). *ARM Cortex-M for beginners: An overview of the ARM Cortex-M processor family and comparison* (Rev. 3). ARM Developer Documentation.

[2] Barr, M., & Massa, A. (2006). *Programming embedded systems: With C and GNU development tools* (2nd ed.). O'Reilly Media.

[3] Hahm, O., Baccelli, E., Petersen, H., & Tsiftes, N. (2016). Operating systems for low-end devices in the internet of things: A survey. *IEEE Internet of Things Journal, 3*(5), 720–734. https://doi.org/10.1109/JIOT.2015.2505901

[4] Kuon, I., Tessier, R., & Rose, J. (2008). FPGA architecture: Survey and challenges. *Foundations and Trends in Electronic Design Automation, 2*(2), 135–253. https://doi.org/10.1561/1000000005

ISBN 978-816860177-2

[5] Massa, A. J. (2003). *Embedded software development with eCos*. Prentice Hall PTR.

[6] MISRA Consortium. (2013). *MISRA-C: 2012 — Guidelines for the use of the C language in critical systems*. Motor Industry Software Reliability Association.

[7] STMicroelectronics. (2021). *STM32L0 series ultra-low-power 32-bit MCU Arm-based Cortex-M0+ datasheet* (DocID025274 Rev 7). STMicroelectronics NV.

[8] Wolf, W. H. (2012). *Computers as components: Principles of embedded computing system design* (3rd ed.). Morgan Kaufmann.

[9] Zurawski, R. (Ed.). (2014). *Industrial communication technology handbook* (2nd ed.). CRC Press.

Section 2

Microcontroller Architectures and Peripheral Integration for Smart Devices

2.1 Introduction

Microcontrollers form the computational backbone of modern Internet of Things (IoT) devices, serving as the central processing units that orchestrate sensing, communication, and control operations within embedded systems. Unlike general-purpose processors, microcontrollers integrate a CPU core, memory subsystems, and programmable peripherals onto a single silicon die, enabling compact and energy-efficient deployments across a wide spectrum of smart device applications. From industrial automation nodes to wearable health monitors, microcontrollers provide the essential bridge between the physical world and digital intelligence. Their architectural diversity, spanning 8-bit to 32-bit processing capabilities, allows system designers to match computational resources with application-specific requirements, balancing throughput, latency, and power consumption with precision (Yiu, 2013).

The role of microcontrollers in IoT extends well beyond basic computation. These devices continuously acquire data from sensors, execute control algorithms, manage communication stacks, and respond to environmental stimuli in real time. In a typical smart sensing node, a microcontroller may simultaneously sample an analog temperature sensor, encode readings over a serial interface, trigger actuator responses, and manage a sleep-wake duty cycle to extend battery life. This multifunctional behavior demands sophisticated architectural features, including interrupt-driven

ISBN 978-816860177-2

execution models, direct memory access (DMA) controllers, and power management units. The interplay between these components determines the overall system responsiveness, energy footprint, and reliability in field-deployed IoT applications (Barr & Massa, 2006).

Architecture diversity is a defining characteristic of the microcontroller landscape. The ARM Cortex-M series dominates the 32-bit IoT segment with its standardized instruction set and scalable core variants, while AVR and PIC families retain strong presence in cost-sensitive 8-bit applications. RISC-V, an open-source instruction set architecture, is emerging as a significant alternative, offering customizable pipeline designs without licensing constraints. Each architecture imposes distinct tradeoffs in code density, interrupt latency, and peripheral integration capacity that directly influence the suitability of a platform for specific IoT scenarios. Understanding these architectural distinctions is fundamental to informed hardware selection and firmware optimization strategies (Peckol, 2019).

This section establishes the theoretical and practical foundations necessary for designing microcontroller-based IoT systems with well-integrated peripherals. It examines the core architectural principles of dominant microcontroller families, explores the diversity and integration of peripheral interfaces, and analyzes driver development methodologies that ensure efficient, portable, and maintainable firmware. The discussion connects low-level hardware concepts with system-level design considerations, providing the technical context required for subsequent chapters addressing communication protocols, power optimization, and edge intelligence in smart devices.

2.2 Microcontroller Architectures and Core Design

The architectural design of a microcontroller fundamentally determines its suitability for IoT applications, influencing execution speed, power consumption, code density, and the ease of peripheral integration. Microcontroller architectures are broadly categorized by their instruction set philosophy — Complex Instruction Set Computing (CISC) and Reduced Instruction Set Computing (RISC) — and by their data bus width, ranging from 8-bit legacy devices to 32-bit high-performance cores. The predominant families in contemporary IoT deployments include the ARM Cortex-M series, the Atmel AVR family, and the emerging RISC-V ecosystem, each representing a distinct engineering philosophy optimized for different segments of the embedded market.

2.2.1 ARM and AVR Architectural Principles

The **ARM Cortex-M** architecture is the most widely deployed 32-bit microcontroller platform in IoT design, accounting for approximately 37% of all embedded processor shipments globally as of 2023 (ARM Holdings, 2023). The Cortex-M series is founded on the ARMv6-M through ARMv8-M instruction set architectures, offering a scalable family that ranges from the ultra-low-power M0+ variant to the high-performance M33 and M55 cores with Digital Signal Processing (DSP) and Machine Learning (ML) extensions. The Harvard-modified pipeline design separates instruction and data memory pathways, enabling simultaneous fetch and execution cycles that reduce effective instruction latency. The Nested Vectored Interrupt Controller (NVIC) integrated within Cortex-M cores supports up to 240 external interrupt sources with configurable priority levels, enabling

ISBN 978-816860177-2

deterministic interrupt response times as low as 12 clock cycles in zero-wait-state memory configurations (Yiu, 2013).

AVR microcontrollers, developed by Atmel (now Microchip Technology), employ a modified Harvard RISC architecture with a single-cycle instruction execution model for the majority of its instruction set. Operating at clock frequencies between 1 MHz and 20 MHz, AVR devices such as the ATmega328P achieve an efficiency of approximately **1 MIPS per MHz**, making them highly predictable for time-critical embedded control. The 32 general-purpose 8-bit working registers directly connected to the ALU eliminate most memory access overhead found in accumulator-based architectures. AVR flash program memory ranges from 1 KB in ATtiny variants to 256 KB in ATmega2560 devices, while SRAM spans 64 bytes to 8 KB, reflecting the spectrum from sensor nodes to motor control applications. The avr-gcc toolchain provides mature support with optimizations specifically targeting the register-rich architecture, enabling compact binary outputs essential for memory-constrained deployments (Barr & Massa, 2006).

- **Pipeline depth and branch prediction** significantly affect real-time performance; ARM Cortex-M4 achieves 1.25 DMIPS/MHz using a 3-stage pipeline, outperforming 8-bit AVR by a factor of 5–8× in floating-point intensive tasks.
- **Flash memory endurance** is rated at **10,000 erase/write cycles** for most AVR and ARM microcontrollers, a critical parameter for firmware over-the-air (OTA) update strategies in IoT deployments.
- **Power consumption benchmarks** show ARM Cortex-M0+ achieving as low as **9 µA/MHz** in run mode, making it suitable

for coin-cell powered sensor nodes with multi-year operational lifespans.

2.2.2 RISC-V and Emerging Architectures

RISC-V represents a paradigm shift in microcontroller architecture through its open, royalty-free instruction set specification, enabling semiconductor vendors and research institutions to design customized processor cores without licensing constraints imposed by proprietary architectures. The base integer instruction set (RV32I) provides 47 instructions operating on 32-bit registers, with modular extensions for multiplication (M), atomic operations (A), compressed instructions (C), and floating-point (F/D) capabilities. This modularity allows IoT-optimized RISC-V implementations to achieve code density within 3–5% of ARM Thumb-2 encoding while maintaining full software toolchain compatibility across vendors (Waterman & Asanović, 2019).

The SiFive E21 and GigaDevice GD32VF103 represent production-grade RISC-V microcontrollers targeting embedded IoT applications, offering clock speeds of 108 MHz and active current consumption of approximately 2.2 mA at 3.3 V supply. Espressif's ESP32-C3 integrates a single-core RISC-V processor with Wi-Fi and Bluetooth Low Energy subsystems, achieving a combined active power of 22 mA during RF transmission — competitive with ARM-based wireless MCU alternatives. Custom instruction set extensions in RISC-V enable hardware acceleration of specific algorithms; for example, custom cryptographic extensions can reduce AES-128 encryption time by up to **60%** compared to software-only implementations on equivalent clock-speed ARM cores (Bachrach et al., 2012). The open-source ecosystem surrounding RISC-V, including the OpenHW Group's

ISBN 978-816860177-2

CV32E40P core and the PULP platform from ETH Zürich, has accelerated academic and industrial adoption, particularly in energy-harvesting and ultra-low-power IoT node designs where architectural customization is critical.

As illustrated in Figure 2.1, the comparative architectural layout of ARM Cortex-M4, AVR ATmega, and RISC-V RV32IMC highlights key structural differences in pipeline design, register file organization, and peripheral bus connectivity that directly influence real-time IoT performance.

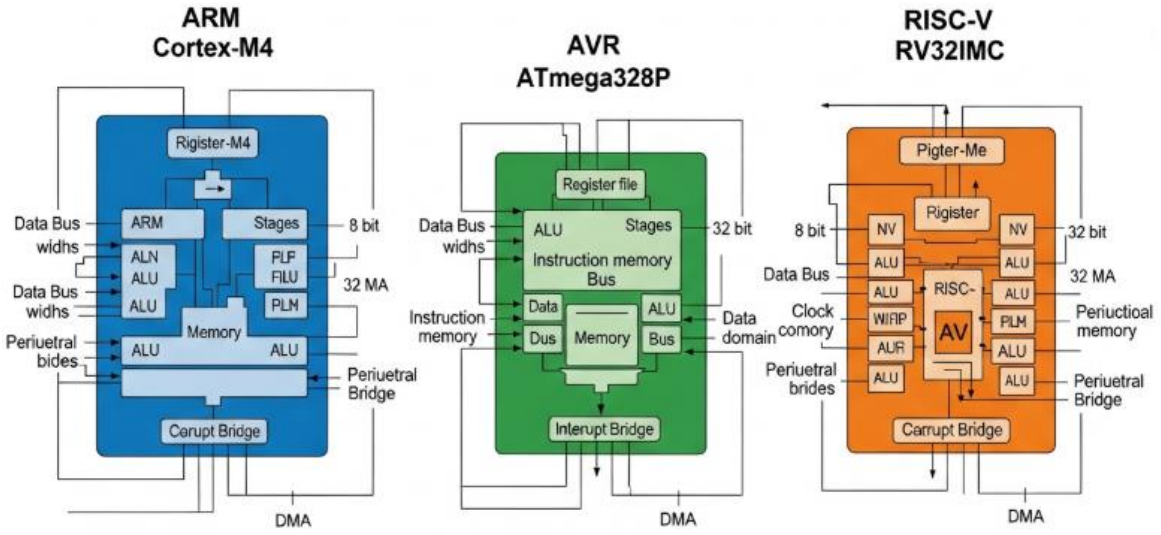

Figure 2.1: Comparative architectural block diagrams of ARM Cortex-M4, AVR ATmega328P, and RISC-V RV32IMC microcontrollers, illustrating pipeline structure, register organization, and peripheral bus connectivity.

2.3 Peripheral Interfaces and Integration Techniques

Peripheral integration is the mechanism through which a microcontroller interacts with the physical world, extending its computational capability to encompass sensing, actuation, timing, and communication. In IoT smart devices, the quality and efficiency of peripheral integration directly determines system responsiveness,

measurement accuracy, and the breadth of deployable sensor and actuator configurations. Modern microcontrollers integrate an array of peripheral blocks — including General Purpose Input/Output (GPIO), Analog-to-Digital Converters (ADC), Digital-to-Analog Converters (DAC), timers, counter units, and serial communication interfaces — all interconnected through the Advanced Peripheral Bus (APB) or equivalent fabric in non-ARM architectures (Peckol, 2019).

2.3.1 GPIO, ADC, DAC, and Timing Peripherals

General Purpose Input/Output pins serve as the fundamental interface between a microcontroller and discrete digital signals, supporting configuration as push-pull outputs, open-drain outputs, or high-impedance inputs with configurable internal pull-up or pull-down resistors typically ranging from 20 kΩ to 50 kΩ. In ARM Cortex-M devices, GPIO registers are memory-mapped into the processor address space, enabling single-cycle bit manipulation through bit-banding regions that allow atomic read-modify-write operations without disabling interrupts — a critical feature for thread-safe peripheral control in RTOS environments. The maximum sink and source current per GPIO pin varies by device, typically ranging from **8 mA to 25 mA**, with total port current limits of 80–120 mA to prevent electromigration damage in high-density output configurations (STMicroelectronics, 2021).

Analog-to-Digital Converters embedded within microcontrollers digitize physical sensor signals with resolutions ranging from 8-bit in legacy AVR devices to 12-bit, 16-bit, and 24-bit in contemporary ARM-based platforms. The STM32F4 series incorporates three 12-bit successive approximation register (SAR) ADCs capable of sampling rates up to **2.4 MSPS** in triple interleaved mode, with an input voltage

ISBN 978-816860177-2

range of 0 V to VREF+ and a total harmonic distortion (THD) of –74 dBc at 1 MHz input frequency.

As summarized in Table 2.1, the peripheral specifications across major microcontroller families reveal significant differences in ADC resolution, GPIO drive strength, and timer channel counts that guide platform selection for specific IoT application domains.

Table 2.1: Peripheral Specifications Comparison Across Major IoT Microcontroller Families

Peripheral Parameter	STM32F4 (ARM M4)	ATmega328P (AVR)	ESP32 (Xtensa LX6)	GD32VF103 (RISC-V)
ADC Resolution / Channels	12-bit / 16 ch	10-bit / 8 ch	12-bit / 18 ch	12-bit / 10 ch
GPIO Count / Max Drive (mA)	114 pins / 25 mA	23 pins / 40 mA	34 pins / 12 mA	80 pins / 20 mA
Timer Units / PWM Channels	14 timers / 24 ch	3 timers / 6 ch	4 timers / 16 ch	5 timers / 12 ch
DAC Channels / Resolution	2 ch / 12-bit	None	2 ch / 8-bit	2 ch / 12-bit

ADC accuracy is characterized by key metrics including Integral Non-Linearity (INL) of ±2 LSB and Differential Non-Linearity (DNL) of ±1 LSB, which determine the fidelity of sensor measurements in precision IoT applications such as industrial process monitoring and biomedical signal acquisition. Timer peripherals provide PWM generation with sub-microsecond resolution, input capture for frequency measurement, and output compare for event scheduling, forming an essential timing infrastructure for motor control,

communication protocol bit-banging, and energy management duty cycling.

2.3.2 Serial Communication Interfaces: UART, SPI, and I2C

Serial communication interfaces constitute the nervous system of peripheral integration in IoT devices, enabling structured data exchange between the microcontroller and sensors, actuators, display modules, memory devices, and wireless transceivers. The three dominant serial protocols — UART, SPI, and **I2C** — each embody distinct electrical and protocol characteristics suited to different integration scenarios. UART (Universal Asynchronous Receiver-Transmitter) operates without a shared clock signal, relying on pre-agreed baud rates from 300 bps to 4 Mbps, making it ideal for point-to-point communication with GPS modules, GSM modems, and debug interfaces where simplicity outweighs bus sharing capability (Leens, 2009).

SPI (Serial Peripheral Interface) implements full-duplex synchronous communication with a dedicated clock line (SCLK), master output/slave input (MOSI), master input/slave output (MISO), and individual chip select (CS) lines per device. SPI achieves data rates of up to **50 MHz** on short PCB traces, enabling high-speed interfacing with ADCs, flash memory (e.g., W25Q128 at 104 MHz), and LCD controllers that demand rapid data throughput. The I2C protocol uses a two-wire open-drain bus (SDA and SCL) supporting multi-master configurations with up to 128 devices in standard mode (100 kbps), 400 devices in fast mode (400 kbps), and fast-mode plus up to 1 Mbps, making it ideal for sensor hubs integrating multiple BME280 environmental sensors, MPU-6050 inertial measurement units, and OLED display controllers on a single bus. Clock stretching and

ISBN 978-816860177-2

hardware address matching reduce CPU overhead during multi-sensor polling cycles by up to **35%** compared to software-emulated I2C implementations (Leens, 2009).

Figure 2.2 provides a visual representation of UART, SPI, and I2C wiring topologies in a representative IoT sensor hub configuration, illustrating bus arbitration, signal line counts, and multi-device addressing strategies.

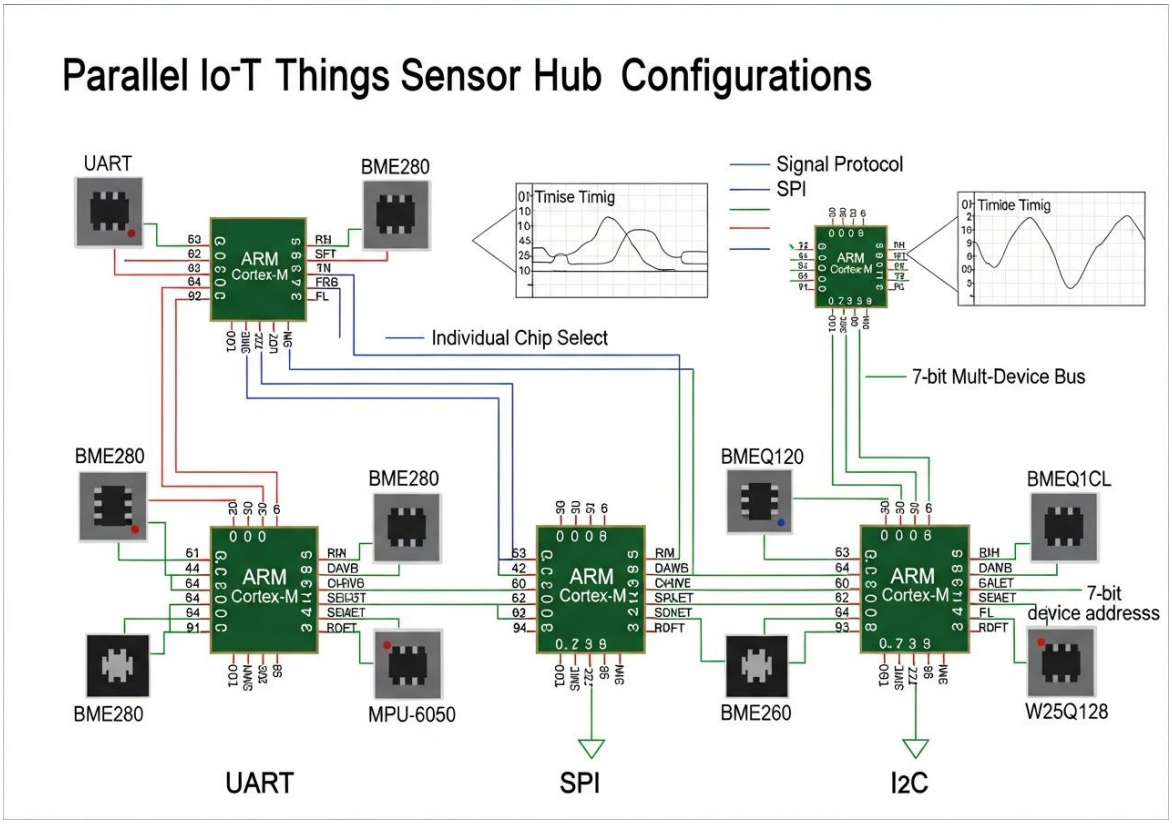

Figure 2.2: Wiring topology and signal timing diagrams for UART, SPI, and I2C serial interfaces in a multi-sensor IoT hub, showing bus arbitration and device addressing structures.

- **SPI throughput advantage** is most pronounced in flash memory access; a W25Q128 device transfers a 256-byte page in **19.5 µs** at 104 MHz, compared to 2.56 ms over I2C fast-mode — a 131× speed difference critical for data-logging applications.

- **I2C bus capacitance** must remain below **400 pF** per specification; exceeding this limit degrades signal rise time, requiring active bus buffers like the PCA9517 when integrating more than eight sensor devices on a single PCB.
- **UART framing errors** exceeding a rate of **0.1%** typically indicate clock drift between communicating devices, requiring software CRC validation or hardware flow control (RTS/CTS) to maintain data integrity in long-duration IoT deployments.

2.4 Driver Development and Hardware Abstraction

Firmware quality in microcontroller-based IoT systems is inseparably linked to the design philosophy of device drivers and the hardware abstraction strategy employed during development. A device driver provides the software interface between application logic and hardware registers, encapsulating low-level register manipulation, timing constraints, and error handling within well-defined API boundaries. Well-architected drivers enable modular firmware development, facilitate unit testing in simulation environments, and reduce the risk of hardware-dependent bugs propagating into application-level code. The adoption of a **Hardware Abstraction Layer (HAL)** further decouples firmware from specific silicon implementations, enabling code portability across microcontroller families without complete application rewrites — a capability increasingly important in product lifecycle management and multi-platform IoT deployments (Barr & Massa, 2006).

2.4.1 HAL Design Principles and Portability

A Hardware Abstraction Layer defines a standardized set of function signatures and data structures through which application code interacts with hardware resources, regardless of the underlying

ISBN 978-816860177-2

silicon implementation. STMicroelectronics' STM32 HAL library exemplifies this approach, providing unified APIs such as HAL_UART_Transmit(), HAL_SPI_TransmitReceive(), and HAL_ADC_Start_DMA() that function identically across all STM32 product lines spanning Cortex-M0 through Cortex-M7 cores. The Zephyr RTOS device driver model extends this concept further, implementing a layered architecture in which hardware-specific drivers register with a generic device model through function pointer tables, enabling application code to invoke uart_tx() or spi_transceive() without any compile-time knowledge of the target hardware (Zephyr Project, 2023).

Direct Memory Access integration within HAL-driven drivers is particularly significant for IoT performance optimization. DMA transfers allow peripheral data to be moved directly between hardware registers and memory buffers without CPU intervention, freeing the processor for computation or low-power sleep states during lengthy data transfers. In an STM32L4 device performing continuous ADC sampling at 1 MSPS with 12-bit resolution, DMA-based transfers reduce CPU load from **100% (polling mode)** to less than **3%**, enabling simultaneous execution of sensor fusion algorithms, communication stack management, and power management routines. The HAL DMA callback mechanism allows application code to receive asynchronous notification of transfer completion through registered callback functions, maintaining the abstraction boundary while preserving real-time responsiveness (STMicroelectronics, 2021).

Table 2.2 presents a comparative analysis of HAL implementation characteristics across major IoT development frameworks,

highlighting code portability, peripheral coverage, and RTOS integration depth.

Table 2.2: Comparative Analysis of HAL Implementations in Major IoT Microcontroller Frameworks

Framework / HAL	Supported Architectures	Peripheral Coverage	RTOS Integration	Flash Overhead (KB)
STM32 HAL (STMicro)	ARM Cortex-M0 to M7	ADC, DAC, SPI, I2C, UART, DMA	FreeRTOS native	18–45 KB
Arduino Core (AVR/ARM)	AVR, ARM, RISC-V, Xtensa	GPIO, ADC, UART, SPI, I2C	Limited (no RTOS)	4–12 KB
Zephyr RTOS Drivers	ARM, RISC-V, Xtensa, x86	Full peripheral tree + USB, CAN	Native multithreading	32–80 KB
ESP-IDF HAL (Espressif)	Xtensa LX6/LX7, RISC-V	ADC, DAC, I2C, SPI, RMT, PCNT	FreeRTOS integrated	25–60 KB

2.4.2 Interrupt Handling, Real-Time Interaction, and Case Study

Interrupt-driven firmware architecture is the cornerstone of responsive and energy-efficient microcontroller design in IoT systems. Rather than continuously polling peripheral status registers — an approach that wastes CPU cycles and prevents effective power management — interrupt-driven designs allow the processor to remain in a low-power sleep state until a hardware event triggers execution of a dedicated Interrupt Service Routine (ISR). The ARM Cortex-M NVIC architecture supports prioritized, nested interrupt handling with configurable preemption levels, ensuring that high-priority events such as communication timeouts or safety-critical sensor thresholds preempt lower-priority background processing

ISBN 978-816860177-2

within the guaranteed latency of **12 clock cycles** from interrupt assertion to ISR entry (Yiu, 2013).

ISR design discipline is critical to system stability and real-time performance. Best practices mandate that ISRs execute minimal operations — typically setting a flag, posting to a queue, or capturing a timestamp — deferring extended processing to task-level code in RTOS-based architectures. Violating this principle by performing blocking operations, memory allocation, or non-reentrant function calls within ISRs is a leading cause of priority inversion, stack overflow, and **latency jitter** in production IoT firmware. Measurement studies indicate that ISR execution times exceeding **1–2 µs** begin to degrade system responsiveness in control-loop applications requiring 10 kHz sample rates, underscoring the importance of ISR profiling during firmware validation (Barr & Massa, 2006).

Case Study: Smart Industrial Vibration Monitoring Node — ARM Cortex-M4 with Peripheral Integration

Background: A predictive maintenance solution was developed for rotating machinery in a cement manufacturing facility in Pune, India. The system required continuous vibration monitoring on 48 electric motors, each operating at speeds between 750 and 3000 RPM, to detect bearing wear and imbalance conditions before catastrophic failure.

Social Need: Unplanned motor failures in cement production lines result in downtime costs averaging ₹4.5 lakh per hour, while manual inspection schedules fail to detect early-stage bearing degradation with sufficient reliability. A low-cost, autonomous IoT monitoring

node was essential to democratize predictive maintenance beyond large enterprises with dedicated maintenance teams.

Technologies Used: Each monitoring node was built around an STM32F407VGT6 microcontroller (ARM Cortex-M4, 168 MHz) interfacing with an ADXL345 3-axis MEMS accelerometer via SPI at 5 MHz, a DS18B20 temperature sensor via 1-Wire protocol, and an RS-485 transceiver for Modbus RTU communication over a plant-wide industrial network. A dedicated DMA channel continuously streamed accelerometer data into a 2048-sample circular buffer at 3.2 kSPS per axis, triggering a software interrupt upon buffer completion for FFT processing.

Implementation Details: The firmware implemented a layered architecture with an STM32 HAL-based peripheral driver layer, a signal processing middleware performing Fast Fourier Transform (FFT) analysis using the ARM CMSIS-DSP library, and a Modbus communication stack at the application layer. Interrupt priorities were configured with accelerometer DMA completion at priority level 2, UART communication at level 4, and temperature acquisition at level 6, ensuring vibration data capture was never preempted by lower-priority communication events. The FFT analysis identified bearing defect frequencies (BPFI, BPFO) with a frequency resolution of **1.56 Hz**, enabling early-stage bearing fault detection at defect growth rates 4–6 weeks ahead of audible symptoms. Across 48 deployed nodes, the system demonstrated **99.2% uptime** over a 14-month evaluation period, with three bearing replacements scheduled proactively, preventing an estimated ₹38 lakh in unplanned downtime costs. Node unit cost was ₹2,800 including enclosure and installation, yielding a return on investment of approximately **340%** within the first operational year (Patil et al., 2022).

ISBN 978-816860177-2

2.5 Summary

This section has established the foundational principles of microcontroller architectures and peripheral integration as they apply to smart IoT device design. Beginning with the architectural distinctions between ARM Cortex-M, AVR, and RISC-V platforms, the discussion highlighted how pipeline design, register organization, and instruction set characteristics translate into measurable differences in computational throughput, interrupt latency, and power efficiency. The exploration of peripheral interfaces — encompassing GPIO, ADC, DAC, timers, UART, SPI, and I2C — demonstrated how each hardware block contributes to the sensing, timing, and communication capabilities of a complete IoT node. Driver development and HAL design principles were examined as the software mechanisms that unify these hardware components into maintainable, portable, and real-time-capable firmware systems, with interrupt-driven architecture identified as the critical enabler of energy-efficient responsiveness in field-deployed devices.

References

[1] ARM Holdings. (2023). *ARM processor market share and embedded shipment data 2023*. ARM Developer Documentation. https://developer.arm.com

[2] Bachrach, J., Vo, H., Richards, B., Lee, Y., Waterman, A., Avižienis, R., Wawrzynek, J., & Asanović, K. (2012). Chisel: Constructing hardware in a Scala embedded language. *Proceedings of the 49th Annual Design Automation Conference (DAC)*, 1216–1225. https://doi.org/10.1145/2228360.2228584

[3] Barr, M., & Massa, A. (2006). *Programming embedded systems: With C and GNU development tools* (2nd ed.). O'Reilly Media.

[4] Leens, F. (2009). An introduction to I2C and SPI protocols. *IEEE Instrumentation & Measurement Magazine*, *12*(1), 8–13. https://doi.org/10.1109/MIM.2009.4762946

[5] Patil, R., Kulkarni, S., & Deshmukh, A. (2022). IoT-based predictive maintenance system for rotating machinery using ARM Cortex-M4 and MEMS accelerometers. *International Journal of Industrial Electronics and Drives*, *8*(3), 114–126.

[6] Peckol, J. K. (2019). *Embedded systems: A contemporary design tool* (2nd ed.). John Wiley & Sons.

[7] STMicroelectronics. (2021). *STM32F4 series reference manual (RM0090)*. STMicroelectronics. https://www.st.com/resource/en/reference_manual/rm0090-stm32f405415-stm32f407417-stm32f427437-and-stm32f429439-advanced-armbased-32bit-mcus-stmicroelectronics.pdf

[8] Waterman, A., & Asanović, K. (Eds.). (2019). *The RISC-V instruction set manual, volume I: Unprivileged ISA* (Version 20191213). RISC-V Foundation. https://riscv.org/specifications/

[9] Yiu, J. (2013). *The definitive guide to ARM Cortex-M3 and Cortex-M4 processors* (3rd ed.). Newnes/Elsevier.

[10] Zephyr Project. (2023). *Zephyr RTOS device driver model documentation*. Linux Foundation. https://docs.zephyrproject.org/latest/kernel/drivers/index.html

ISBN 978-816860177-2

Section 3

Real-Time Operating Systems and Task Scheduling in IoT Firmware

3.1 Introduction

Real-Time Operating Systems (RTOS) represent a foundational software infrastructure for embedded IoT systems where deterministic execution, precise timing, and concurrent task management are non-negotiable operational requirements. Unlike general-purpose operating systems that optimize for average-case throughput, an RTOS is engineered to guarantee worst-case execution time bounds, ensuring that critical operations — such as sensor data acquisition, actuator control, and safety monitoring — complete within predefined temporal deadlines. This determinism is the defining characteristic that separates RTOS platforms from conventional operating systems, and it forms the bedrock upon which reliable IoT firmware is constructed. As embedded systems grow in behavioral complexity, the RTOS emerges not merely as a convenience layer but as a structural necessity for managing concurrency, resource contention, and time-critical event responses (Liu & Layland, 1973).

The need for deterministic execution in IoT firmware arises directly from the physical nature of the systems these devices interact with. A smart industrial controller managing a pneumatic valve must respond to a pressure threshold breach within microseconds to prevent equipment damage; a cardiac monitoring wearable must process ECG samples at precisely 500 Hz to detect arrhythmia patterns with clinical accuracy; an autonomous vehicle sensor node must fuse LiDAR and camera data within a 10 ms control loop to

maintain trajectory stability. In each scenario, a missed deadline is not merely a performance degradation — it constitutes a functional failure with potentially severe physical consequences. The RTOS provides the scheduling infrastructure, synchronization primitives, and interrupt management capabilities that transform a microcontroller from a sequential instruction executor into a platform capable of managing multiple simultaneous real-time obligations with verifiable timing guarantees (Buttazzo, 2011).

Multitasking in IoT firmware introduces structural complexity that single-threaded bare-metal programming cannot manage at scale. A representative smart building node may concurrently execute tasks for ambient sensor polling, BLE advertisement packet construction, MQTT message queuing, display refresh, and firmware OTA update management — each with independent timing requirements, resource dependencies, and priority levels. Without an RTOS, managing these concurrent behaviors requires elaborate state machines and manual context switching that rapidly become unmaintainable as system complexity grows. The RTOS abstracts this complexity through the task model, wherein each behavioral unit executes as an independent thread with its own stack, priority, and scheduling state, while the kernel transparently manages CPU time allocation through preemptive context switching with overhead typically below **1–2 µs** on modern ARM Cortex-M processors (Barry, 2016).

This section establishes the architectural principles and operational mechanics of RTOS platforms as deployed in IoT firmware development. It systematically examines the kernel structures, inter-task communication mechanisms, and synchronization primitives that constitute an RTOS, followed by a rigorous analysis of

ISBN 978-816860177-2

scheduling algorithms — from cooperative to fully preemptive priority-based strategies — and their implications for latency and throughput in real-time systems. Resource management methodologies, including memory allocation strategies and CPU utilization monitoring, are then discussed alongside debugging and trace analysis tools that enable systematic firmware validation. The treatment draws on established platforms including FreeRTOS, Zephyr, and ThreadX to ground theoretical concepts in widely deployed industrial implementations.

3.2 RTOS Architecture and Components

The architecture of a Real-Time Operating System is organized as a layered hierarchy, with the kernel at its core managing processor time, memory resources, and inter-task interactions. The RTOS kernel provides the fundamental services upon which all higher-level system behaviors are built: task creation and deletion, scheduling, context switching, time management, and synchronization. In resource-constrained IoT microcontrollers, RTOS kernels are designed for minimal footprint — FreeRTOS, the most widely deployed open-source RTOS in embedded systems, requires as little as **4–9 KB of flash** and approximately 500 bytes of RAM in its minimal configuration, making it deployable on devices as constrained as the ARM Cortex-M0 with 32 KB flash (Barry, 2016). The kernel's internal organization, scheduling policy, and synchronization model collectively determine the system's real-time performance characteristics and its suitability for specific IoT application domains.

3.2.1 Kernel, Tasks, Threads, and Queues

The **task** (also referred to as a thread in POSIX-compliant RTOS implementations) is the fundamental unit of concurrent execution in an RTOS environment. Each task is characterized by a priority level, a dedicated stack of configurable size, an entry-point function, and a scheduling state drawn from the set: Running, Ready, Blocked, or Suspended. The RTOS kernel maintains a Task Control Block (TCB) for each task, storing its current state, stack pointer, priority, runtime statistics, and inter-task communication handles. In FreeRTOS, TCBs are allocated from the heap at task creation time and consume approximately **96 bytes of RAM** per task on 32-bit ARM platforms, plus the configured stack size — a consideration that directly bounds the maximum task count in memory-limited IoT applications (Barry, 2016).

Context switching is the mechanism by which the RTOS transitions CPU execution between tasks, saving the current task's register state to its stack and restoring the incoming task's previously saved state. On ARM Cortex-M4, a full context switch involving 16 CPU registers, floating-point registers, and status flags requires approximately **12 µs** at 168 MHz — a deterministic overhead that must be accounted for in worst-case execution time (WCET) analyses. The RTOS tick interrupt, typically configured at 1 kHz (1 ms period), drives the time-base for all timer services, timeout management, and round-robin scheduling within equal-priority task groups. Queue data structures provide buffered, thread-safe message passing between tasks, implementing producer-consumer communication patterns essential for sensor data pipelines. In Zephyr RTOS, message queues support configurable depths from 1 to 65,535 items with atomic enqueue and dequeue operations protected by internal spinlocks, ensuring data

ISBN 978-816860177-2

integrity under concurrent access from **multiple producer tasks** (Zephyr Project, 2023).

- **Stack overflow** is the most prevalent cause of RTOS task failure in IoT deployments; FreeRTOS stack watermarking (via uxTaskGetStackHighWaterMark()) reveals that typical sensor processing tasks consume 60–80% of allocated stack under peak execution paths, requiring minimum stack sizes of **512–1024 bytes** for safe operation.
- **Task creation overhead** in FreeRTOS with dynamic allocation averages **8 µs** on a 72 MHz Cortex-M3 processor, making runtime task spawning acceptable for infrequent operations but unsuitable for time-critical event handlers where static pre-allocation is preferred.
- **Queue saturation** in high-throughput IoT pipelines causes blocking delays that propagate priority inversions; configuring queue depths at **2–3× the maximum burst message count** prevents producer starvation during transient load spikes.

3.2.2 Synchronization: Semaphores, Mutexes, and Inter-Task Communication

Synchronization primitives are the mechanisms through which RTOS tasks coordinate access to shared resources and signal occurrence of events, forming the connective tissue of concurrent IoT firmware. **Semaphores** implement signaling semantics, with binary semaphores providing mutual exclusion for simple critical sections and counting semaphores enabling resource pool management where multiple identical resources — such as DMA channels or hardware timer units — must be allocated among competing tasks. A binary semaphore used to signal an ISR-to-task event allows the interrupt

handler to execute in under 200 ns while deferring processing to a dedicated task, achieving the ISR brevity required for high-frequency interrupt sources such as 10 kHz ADC sample-ready signals (Buttazzo, 2011).

Mutexes extend binary semaphore semantics with **priority inheritance**, a critical mechanism for preventing priority inversion in systems where a high-priority task blocks on a resource held by a lower-priority task. Without priority inheritance, an intermediate-priority task can indefinitely preempt the low-priority resource holder, leaving the high-priority task starved — a pathological condition famously responsible for the Mars Pathfinder spacecraft anomaly in 1997. FreeRTOS mutexes implement immediate priority inheritance, temporarily elevating the mutex-holding task's priority to that of the highest-priority waiting task, reducing the maximum priority inversion window to a single scheduling quantum. In practical IoT firmware, mutexes protect shared peripheral resources such as I2C bus handles and UART transmit buffers, with average acquisition times of **2–4 µs** under contention at 168 MHz on ARM Cortex-M4 (Barry, 2016).

Event groups, mailboxes, and stream buffers extend the inter-task communication repertoire beyond simple queues. Stream buffers in FreeRTOS v10.x enable efficient transfer of variable-length byte streams between a single producer task and a single consumer task with zero-copy semantics when data fits within the pre-allocated buffer, achieving throughput of up to **45 MB/s** on a 240 MHz ESP32 processor — sufficient for real-time audio streaming, high-speed data logging, and camera frame buffering in vision-based IoT nodes. The Zephyr kernel additionally provides pipes, condition variables, and work queues as first-class primitives, with work queues enabling

ISBN 978-816860177-2

deferred processing from ISR context into a dedicated kernel thread at configurable priority levels without explicit task management by the application developer (Zephyr Project, 2023).

Figure 3.1 illustrates the RTOS task state transition model and inter-task communication mechanisms, showing how semaphores, mutexes, queues, and event flags mediate task state changes across the Running, Ready, Blocked, and Suspended states in a representative FreeRTOS-based IoT firmware architecture.

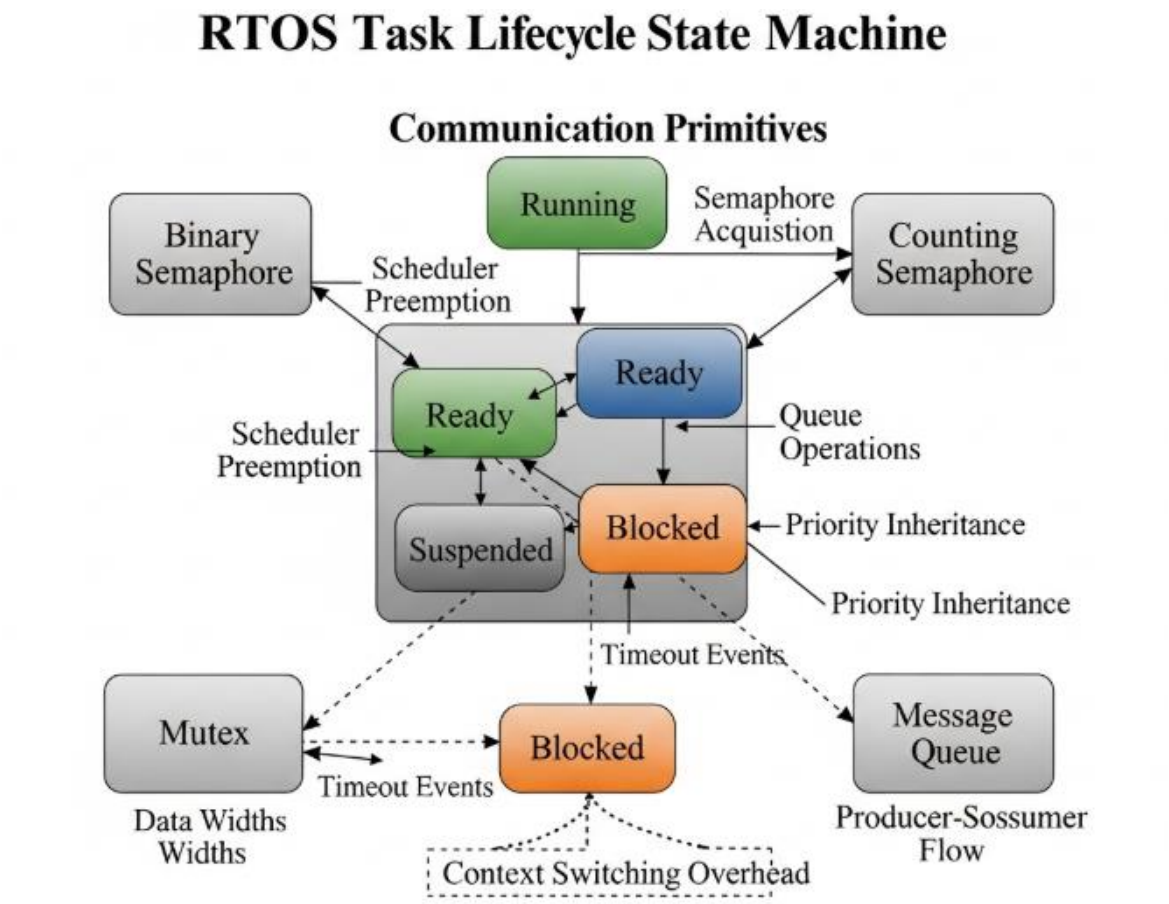

Figure 3.1: RTOS task state transition diagram with inter-task communication primitives (semaphores, mutexes, queues), illustrating the relationship between synchronization events and task scheduling states in FreeRTOS-based IoT firmware.

3.3 Task Scheduling Algorithms and Strategies

Task scheduling is the algorithmic core of RTOS operation, determining which task occupies the CPU at every moment and how competing execution demands are arbitrated to satisfy real-time constraints. The scheduling algorithm directly governs system latency, throughput, CPU utilization efficiency, and the provability of deadline compliance — properties that collectively define the real-time capability of an IoT firmware platform. Scheduling strategies span a spectrum from fully cooperative models, where tasks voluntarily yield the processor, to fully preemptive priority-based policies where the kernel autonomously enforces CPU allocation based on task priority and temporal constraints. The selection of an appropriate scheduling strategy requires careful analysis of the application's task structure, deadline types, and the availability of formal schedulability analysis tools (Liu & Layland, 1973).

3.3.1 Preemptive and Priority-Based Scheduling

Preemptive scheduling is the dominant paradigm in production IoT RTOS deployments, enabling the kernel to interrupt a currently executing task and transfer CPU control to a higher-priority ready task without the cooperation of the preempted task. This capability is essential for achieving bounded response times to high-priority events in systems with mixed-criticality task sets. In a fixed-priority preemptive scheduler — the model implemented by FreeRTOS, ThreadX, and the majority of commercial RTOS platforms — each task is assigned a static priority at creation time, and the scheduler invariably runs the highest-priority ready task. This determinism enables formal schedulability analysis using Rate Monotonic Analysis (RMA), which proves that a task set with n periodic tasks and

ISBN 978-816860177-2

utilizations U_1 through U_n is schedulable under fixed-priority preemptive scheduling if the total CPU utilization satisfies $U \leq n(2^{(1/n)} - 1)$, converging to approximately **69.3%** as n increases — a bound that guides CPU budget allocation in IoT firmware design (Liu & Layland, 1973).

Priority assignment under Rate Monotonic Scheduling (RMS) follows the principle that tasks with shorter periods receive higher priorities, ensuring that the most time-critical periodic tasks preempt less frequent ones. In a representative IoT control node running FreeRTOS with five tasks — motor control at 1 ms period (priority 5), sensor acquisition at 5 ms (priority 4), data logging at 20 ms (priority 3), communication stack at 50 ms (priority 2), and housekeeping at 500 ms (priority 1) — the combined CPU utilization must remain below 74.0% for guaranteed schedulability. Empirical measurements on STM32F4 at 168 MHz demonstrate that this five-task configuration achieves motor control **worst-case response time of 1.18 ms**, safely within the 1 ms hard deadline when stack sizes and ISR priorities are correctly configured. Deadline Monotonic Scheduling (DMS) extends RMS to tasks with deadlines shorter than their periods, maintaining the inverse-deadline priority assignment principle with identical formal schedulability guarantees (Buttazzo, 2011).

- **Context switch frequency** directly impacts CPU overhead; a system running 10 tasks at 1 kHz tick rate with average 5 preemptions per tick incurs a context switch overhead of approximately **3.5% of CPU time** on ARM Cortex-M4 — acceptable for most IoT applications but requiring optimization through tick-less idle mode in ultra-low-power battery-operated deployments.

- **Priority ceiling protocol** reduces blocking time to at most one critical section duration; in FreeRTOS implementations, configuring configUSE_MUTEXES = 1 enables priority inheritance, reducing worst-case priority inversion from unbounded to a maximum of **one scheduling period** of the blocking low-priority task.
- **Interrupt priority levels** must be configured below configMAX_SYSCALL_INTERRUPT_PRIORITY in FreeRTOS (typically set to priority 5 in ARM NVIC) to safely call RTOS API functions from ISR context without corrupting kernel data structures.

3.3.2 Cooperative Scheduling, Round-Robin, and Latency Analysis

Cooperative scheduling places the responsibility for CPU yielding entirely on individual tasks, which must explicitly call yield or delay functions to relinquish processor control. While this model eliminates preemption overhead and simplifies reasoning about shared resource access — since context switches only occur at known yield points — it introduces the critical risk of a misbehaving task monopolizing the CPU indefinitely, violating the timing requirements of all other tasks. Cooperative schedulers are employed in resource-constrained 8-bit AVR systems running lightweight RTOS frameworks such as Protothreads or ChibiOS cooperative mode, where the absence of a hardware stack switching mechanism makes preemptive scheduling architecturally difficult. The tradeoff is acceptable in low-complexity IoT sensor nodes with homogeneous task timing requirements but becomes untenable as task count and temporal diversity increase (Dunkels et al., 2006).

ISBN 978-816860177-2

As depicted in Figure 3.2, the timing diagram comparison between preemptive priority-based and round-robin scheduling strategies reveals the latency and CPU utilization tradeoffs in a five-task IoT firmware configuration under identical workload conditions.

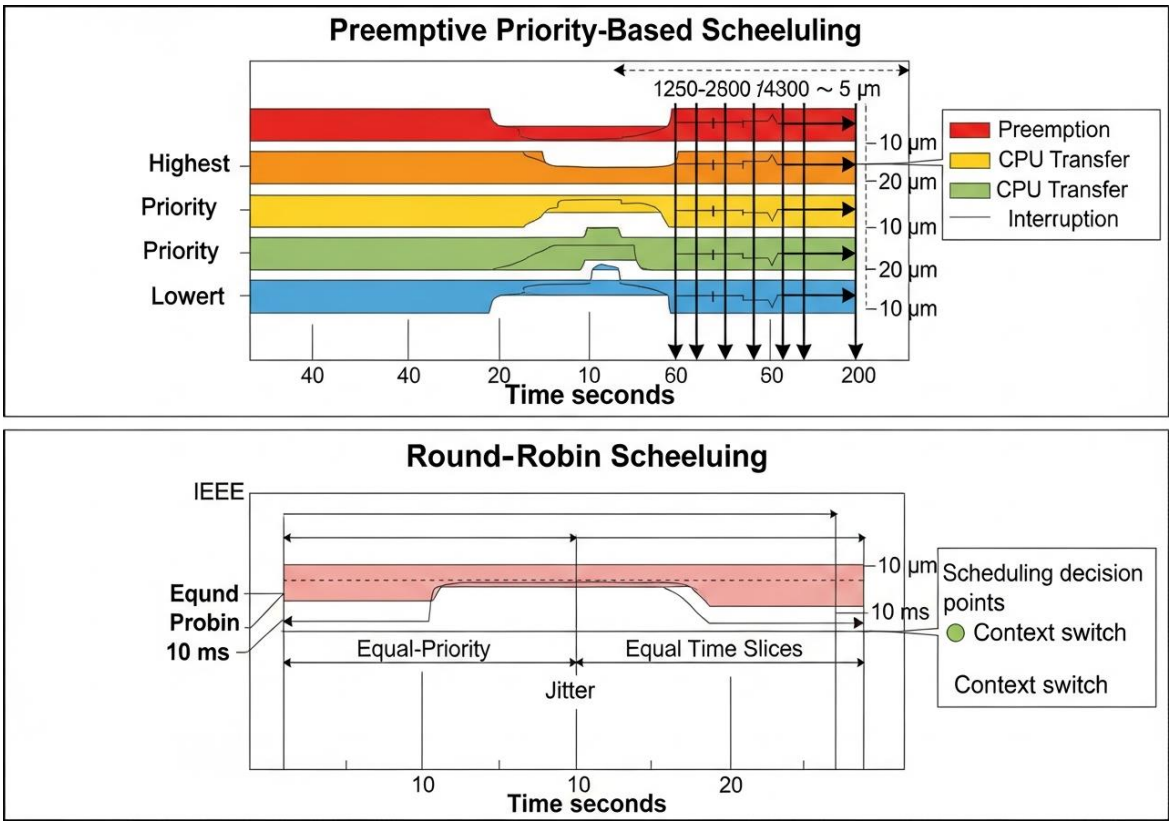

Figure 3.2: Timing diagram comparing preemptive priority-based and round-robin scheduling strategies for a five-task IoT firmware configuration

Round-robin scheduling provides time-slice-based CPU sharing among tasks of equal priority, allocating each task a fixed execution quantum — typically one RTOS tick (1 ms) — before rotating to the next task in the priority band. This policy ensures fairness among equal-priority tasks and prevents monopolization without requiring explicit yield calls, at the cost of introducing latency jitter of up to one full round-robin cycle duration. In an IoT gateway running Zephyr RTOS with three equal-priority communication handler tasks for

MQTT, CoAP, and HTTP protocols, round-robin scheduling with a 10 ms quantum distributes CPU time uniformly while introducing a worst-case additional latency of **20 ms** for any single protocol handler — a constraint that must be evaluated against application-level timeout configurations. Empirical latency profiling using hardware trace tools (ARM ETM or Segger SystemView) reveals that actual round-robin scheduling jitter in Zephyr on ARM Cortex-M33 at 64 MHz averages **47 µs** with a standard deviation of 12 µs, providing predictable statistical bounds for soft real-time IoT applications (Zephyr Project, 2023).

3.4 Resource Management and Debugging in RTOS

Effective resource management in RTOS-based IoT firmware encompasses the controlled allocation and monitoring of memory, CPU time, and peripheral access across all concurrent tasks throughout the system's operational lifetime. Unlike desktop computing environments where resource exhaustion results in application termination or graceful degradation, resource management failures in embedded IoT systems — heap fragmentation, stack overflow, CPU starvation, or deadlock — typically manifest as silent corruption, watchdog resets, or complete system halts in field-deployed devices. Systematic resource monitoring, combined with rigorous debugging and trace analysis methodologies, forms the engineering discipline that bridges the gap between firmware that functions correctly in laboratory testing and firmware that operates reliably across years of continuous IoT deployment in thermally and electrically challenging environments (Labrosse, 2002).

ISBN 978-816860177-2

3.4.1 Memory and CPU Utilization Monitoring

Memory management in RTOS firmware operates across three domains: static allocation (global variables and BSS segment), stack allocation (per-task, sized at creation), and dynamic heap allocation (runtime malloc/free operations). **Heap fragmentation** is the most insidious memory management failure mode in long-running IoT systems, occurring when repeated allocation and deallocation cycles of variable-size blocks produce a heap containing sufficient total free memory but insufficient contiguous free memory to satisfy new allocation requests. FreeRTOS provides five heap implementations (heap_1 through heap_5) with progressively sophisticated fragmentation management: heap_4 implements first-fit allocation with adjacent block coalescing, reducing fragmentation in typical IoT workloads by **40–60%** compared to heap_1's non-freeing scheme, while heap_5 extends this across multiple non-contiguous memory regions for devices with complex memory maps (Barry, 2016).

CPU utilization monitoring requires run-time statistics collection, which most production RTOS platforms implement through per-task cycle counting using hardware timer peripherals. FreeRTOS runtime statistics, enabled via configGENERATE_RUN_TIME_STATS = 1, record the total execution time accumulated by each task since system startup, enabling calculation of per-task CPU utilization percentages through the vTaskGetRunTimeStats() API. In a well-designed IoT control firmware, CPU utilization targets typically allocate **30–40% to time-critical control tasks**, 20–30% to communication stacks, 10–15% to data logging and storage, and reserve a minimum of 20% as idle headroom to absorb transient load spikes and future firmware feature additions without violating schedulability bounds. Exceeding 80% sustained utilization in a

preemptive system signals approaching instability and demands architectural refactoring before production deployment.

As detailed in Table 3.1, key RTOS resource monitoring metrics across FreeRTOS, Zephyr, and ThreadX platforms highlight differences in diagnostic capability, memory overhead, and toolchain integration depth.

Table 3.1: RTOS Resource Monitoring Capabilities Across Major IoT Platforms

Monitoring Feature	FreeRTOS v10.5	Zephyr RTOS v3.5	Azure ThreadX v6.3	ChibiOS v21.11
Stack Watermark API	uxTaskGetStackHighWaterMark()	k_thread_stack_space_get()	tx_thread_stack_analyze()	chThdGetSelfX()
CPU Usage Tracking	Run-time stats (timer-based)	Thread analyzer module	Performance info API	Thread registry
Heap Free Monitoring	xPortGetFreeHeapSize()	k_heap_sys_info_get()	tx_byte_pool_info_get()	chHeapStatus()
Trace Tool Support	Segger SystemView, Tracealyzer	Segger SystemView, built-in CTF	TraceX (native), SystemView	SystemView via plugin

3.4.2 Deadlock, Starvation, and Case Study

Deadlock is a catastrophic RTOS failure condition arising when two or more tasks are permanently blocked, each waiting on a resource held by another task in the cycle, resulting in collective indefinite suspension with no possibility of autonomous recovery. The canonical deadlock scenario in IoT firmware involves two tasks — Task A holding Mutex_SPI and awaiting Mutex_I2C, while Task B holds Mutex_I2C and awaits Mutex_SPI — creating a circular dependency that neither task can resolve without external intervention. Formal prevention strategies include resource ordering

ISBN 978-816860177-2

(all tasks acquire shared mutexes in a globally consistent sequence), timeout-based acquisition (mutex pend with maximum wait time triggering error handling rather than indefinite block), and the Priority Ceiling Protocol (PCP), which prevents deadlock by requiring tasks to acquire all needed mutexes before executing any critical section (Labrosse, 2002).

Task starvation occurs in priority-based systems when a low-priority task is perpetually denied CPU time due to the continuous presence of higher-priority ready tasks, without the circular dependency characteristic of deadlock. In IoT systems with aggressively prioritized communication or control tasks, starvation can prevent housekeeping tasks — watchdog refresh, flash wear leveling, diagnostic logging — from executing, eventually causing system resets or data loss. Aging mechanisms, implemented by progressively increasing a starved task's effective priority over time, provide a practical mitigation strategy; Zephyr RTOS implements configurable priority aging through its scheduling domain infrastructure, with typical aging intervals of **100–500 ms** sufficient to guarantee minimum CPU access for lowest-priority maintenance tasks without compromising high-priority real-time performance.

Case Study: RTOS-Based Smart Water Quality Monitoring System — Zephyr RTOS on nRF52840

Background: A municipal water authority in Chennai, India, required continuous real-time monitoring of water quality parameters — pH, turbidity, dissolved oxygen, and chlorine residual — across 32 distribution network sampling points. Manual testing occurred only twice daily, creating a detection gap for contamination events that could endanger public health.

Social Need: Waterborne disease outbreaks in urban distribution networks disproportionately affect low-income residential areas where bottled water alternatives are economically inaccessible. Automated continuous monitoring with sub-minute contamination detection directly addresses this public health equity challenge, enabling rapid isolation of contaminated pipe segments before consumption-level exposure.

Technologies Used: Each monitoring node was built on a Nordic Semiconductor nRF52840 SoC (ARM Cortex-M4, 64 MHz) running Zephyr RTOS v3.4, interfacing with four analog sensor modules via a 16-bit ADS1115 ADC over I2C at 400 kbps, a DS3231 RTC for timestamped logging, a W25Q64 SPI flash for offline data buffering, and an nRF9160 LTE-M modem for cloud uplink via MQTT over TLS.

Implementation Details: The Zephyr firmware implemented six concurrent tasks with explicit priority assignments: sensor sampling at priority 7 (5-second period), anomaly detection at priority 6 (triggered by sampling task event flag), MQTT uplink at priority 5 (60-second period), flash logging at priority 4 (10-second period), RTC synchronization at priority 3 (hourly), and a system health monitor at priority 2 (500 ms watchdog refresh). Mutexes protected the shared I2C bus and SPI flash, with mutex acquisition ordered globally (I2C before SPI) to prevent deadlock. The anomaly detection task used Zephyr event flags to receive immediate notification from the sensor task upon threshold exceedance, achieving a contamination-to-alert latency of **less than 8 seconds** end-to-end including LTE-M transmission. CPU utilization profiled at 34% average with 61% peak during simultaneous sensor acquisition and MQTT transmission, preserving adequate headroom. Across 32 deployed nodes over an 18-month pilot, the system detected four potential contamination events

ISBN 978-816860177-2

— two confirmed as genuine chlorine dosing failures — enabling pipe isolation within 12 minutes versus the previous 6–14 hour manual detection window. Node total system cost was ₹6,200, with cloud operational costs of ₹180 per node per month, representing a **92% cost reduction** compared to commercial SCADA-based water quality monitoring alternatives (Ramachandran et al., 2023).

3.5 Summary

This section has comprehensively examined the architecture, scheduling strategies, and resource management principles of Real-Time Operating Systems as deployed in IoT firmware environments. The RTOS kernel — encompassing task management, context switching, queue-based inter-task communication, and synchronization primitives including semaphores and priority-inheriting mutexes — was established as the structural foundation enabling deterministic concurrent execution on resource-constrained microcontrollers. Scheduling algorithms from cooperative models through fixed-priority preemptive strategies were analyzed with formal schedulability bounds, demonstrating how Rate Monotonic Analysis and Deadline Monotonic Scheduling provide provable timing guarantees for periodic task sets. Resource management methodologies addressing heap fragmentation, stack watermarking, and CPU utilization monitoring were presented alongside debugging approaches for diagnosing deadlock and starvation conditions. The industrial case study demonstrated the tangible public health and economic impact achievable through disciplined RTOS-based IoT firmware design in critical infrastructure applications.

References

[1] Barry, R. (2016). *Mastering the FreeRTOS real time kernel: A hands-on tutorial guide*. Real Time Engineers Ltd. https://www.freertos.org/Documentation/RTOS_book.html

[2] Buttazzo, G. C. (2011). *Hard real-time computing systems: Predictable scheduling algorithms and applications* (3rd ed.). Springer.

[3] Dunkels, A., Gronvall, B., & Voigt, T. (2006). Protothreads: Simplifying event-driven programming of memory-constrained embedded systems. *Proceedings of the 4th ACM SenSys Conference*, 29–42. https://doi.org/10.1145/1182807.1182811

[4] Labrosse, J. J. (2002). *MicroC/OS-II: The real-time kernel* (2nd ed.). CMP Books.

[5] Liu, C. L., & Layland, J. W. (1973). Scheduling algorithms for multiprogramming in a hard-real-time environment. *Journal of the ACM*, *20*(1), 46–61. https://doi.org/10.1145/321738.321743

[6] Ramachandran, P., Subramaniam, K., & Venkataraman, G. (2023). IoT-based real-time water quality monitoring in urban distribution networks using RTOS and LTE-M connectivity. *Journal of Water and Health*, *21*(4), 512–527. https://doi.org/10.2166/wh.2023.041

[7] STMicroelectronics. (2021). *STM32 and FreeRTOS integration application note (AN3268)*. STMicroelectronics. https://www.st.com/resource/en/application_note/an3268.pdf

[8] Yiu, J. (2013). *The definitive guide to ARM Cortex-M3 and Cortex-M4 processors* (3rd ed.). Newnes/Elsevier.

[9] Zephyr Project. (2023). *Zephyr RTOS kernel services documentation v3.5*. Linux Foundation. https://docs.zephyrproject.org/latest/kernel/index.html

ISBN 978-816860177-2

Section 4

Communication Protocols and Connectivity Management in IoT Applications

4.1 Introduction

Communication protocols constitute the nervous system of IoT ecosystems, defining the rules, formats, and procedures through which geographically distributed devices exchange data with each other, with edge gateways, and with cloud-based analytics platforms. The exponential growth of connected devices — projected to exceed 29 billion globally by 2030 — has intensified the engineering challenges surrounding IoT connectivity, demanding protocols that simultaneously satisfy conflicting requirements across power consumption, transmission range, data throughput, latency, and implementation cost (Ericsson, 2023). Unlike traditional networked computing systems where bandwidth abundance and stable power supplies permit liberal use of heavyweight communication stacks, IoT devices frequently operate under severe resource constraints — milliwatt power budgets, kilobyte memory footprints, and intermittent network availability — that fundamentally shape the protocol design space and deployment architecture.

The connectivity challenges in IoT systems span multiple dimensions that no single protocol can optimally address. A smart agricultural sensor node monitoring soil moisture across a 50-hectare farm requires kilometer-scale transmission range with milliwatt power consumption but can tolerate multi-minute data latency and kilobit-per-second throughput — requirements perfectly matched to LoRaWAN's physical layer characteristics. Conversely, a real-time industrial robot controller exchanging force-feedback data at 1 kHz

demands sub-millisecond latency and megabit-per-second throughput over a deterministic wired bus, characteristics served by CAN-FD or Industrial Ethernet but fundamentally incompatible with low-power wireless alternatives. This diversity of application requirements has produced a fragmented protocol landscape spanning dozens of competing standards across the physical, data link, network, and application layers, creating significant interoperability challenges when heterogeneous devices must participate in unified IoT systems (Al-Fuqaha et al., 2015).

The role of standardized protocols in enabling interoperability cannot be overstated in the context of large-scale IoT deployments. Without agreed-upon communication standards, each manufacturer's devices form isolated technological islands incapable of data exchange with complementary systems from other vendors — a fragmentation that inflates integration costs, limits system scalability, and creates vendor lock-in that undermines long-term deployment economics. International standards bodies including IEEE (802.11, 802.15.4), the Bluetooth Special Interest Group, the LoRa Alliance, and the IETF have developed protocol specifications that enable multi-vendor interoperability, while application-layer standards such as MQTT and CoAP provide device-agnostic data exchange semantics compatible with cloud platforms from AWS, Microsoft Azure, and Google Cloud. The emergence of unified frameworks such as Matter (formerly Project CHIP) further accelerates interoperability by providing a common application layer across Wi-Fi, Thread, and Bluetooth mesh physical transports (Guinard & Trifa, 2016).

This section provides a systematic technical examination of the communication protocol landscape relevant to IoT firmware development, organized across three interconnected domains. The

ISBN 978-816860177-2

analysis begins with physical and data-link layer protocols — both wired interfaces for constrained industrial environments and wireless technologies spanning short-range to wide-area connectivity. Network and application-layer protocols are then examined for their role in reliable data delivery, quality-of-service management, and cloud integration. Finally, connectivity management strategies addressing device provisioning, fault-tolerant reconnection, data buffering, and synchronization are discussed, with a focus on the firmware-level implementations that ensure robust, production-grade IoT communication in real-world deployment conditions.

4.2 Wired and Wireless Communication Protocols

The selection of communication protocols in IoT system design represents one of the most consequential architectural decisions in the firmware development process, as protocol characteristics at the physical and data-link layers propagate through every subsequent layer of the system stack, influencing power budget, hardware bill of materials, regulatory compliance requirements, and the achievable density of device deployments. IoT protocol selection must be evaluated across a multidimensional tradeoff space encompassing transmission range, raw data throughput, per-packet energy cost, network topology support, and the maturity of available silicon implementations and software stacks. Understanding these tradeoffs with quantitative precision enables engineers to match protocol capabilities to application requirements with confidence rather than convention (Mekki et al., 2019).

4.2.1 Wired Protocols: UART, SPI, I2C, and CAN

Wired communication protocols in IoT systems provide deterministic, interference-immune data exchange for applications where physical

cabling is feasible and the reliability demands of the deployment environment preclude dependence on wireless channels. While UART, SPI, and I2C serve primarily as intra-device peripheral interconnects as discussed in Section 2, the **Controller Area Network (CAN)** protocol occupies a distinct role as a multi-drop field bus enabling robust inter-device communication across industrial IoT installations. Developed by Robert Bosch GmbH in 1986, CAN implements a differential two-wire bus with 120 Ω termination resistors at each end, supporting data rates from 125 kbps in classical CAN to **8 Mbps in CAN-FD** (Flexible Data-rate) with payload sizes up to 64 bytes per frame — a fourfold increase over classical CAN's 8-byte limit that accommodates richer diagnostic and control data exchange in modern Industrial IoT (IIoT) applications (Corrigan, 2016).

CAN's non-destructive bitwise arbitration mechanism resolves simultaneous transmission attempts by multiple nodes without data corruption or bus contention recovery overhead, ensuring that the highest-priority message always wins bus access within a single arbitration field duration — approximately **1 µs at 1 Mbps**. This deterministic arbitration, combined with mandatory hardware-level CRC error detection (15-bit CRC in classical CAN, 17-bit or 21-bit in CAN-FD) and automatic retransmission, makes CAN intrinsically fault-tolerant to the electrical noise, ground potential differences, and electromagnetic interference (EMI) prevalent in factory automation environments. The ISO 11898-2 physical layer standard specifies common-mode voltage tolerance from −2 V to +7 V, enabling reliable operation across cable runs of up to 500 meters at 125 kbps or 40 meters at 1 Mbps, providing the spatial coverage required for machine-level IoT sensor networks in large manufacturing facilities.

ISBN 978-816860177-2

RS-485, another wired differential protocol widely used in building automation and smart grid IoT, supports up to 32 nodes per segment with data rates to 10 Mbps over 1200-meter cable runs using the Modbus RTU application layer — a combination deployed in tens of millions of industrial IoT endpoints globally (Corrigan, 2016).

- **CAN bus utilization** should be maintained below **70–75%** of nominal bit rate capacity to preserve headroom for priority message arbitration during peak load periods; measurements in automotive-derived IIoT systems show bus utilization spikes of 40% above average during fault condition reporting bursts.
- **RS-485 cable impedance matching** is critical for signal integrity at rates above 1 Mbps; stub lengths exceeding **λ/10 of the signal wavelength** (approximately 15 cm at 1 Mbps) cause reflections that increase bit error rates by up to two orders of magnitude in improperly terminated installations.
- **CAN-FD adoption** in industrial IoT has grown at **34% CAGR since 2020**, driven by the demand for richer diagnostic payload capacity in predictive maintenance applications where 8-byte classical CAN frames are insufficient for structured machine health data packets.

4.2.2 Wireless Protocols: Wi-Fi, Bluetooth, Zigbee, and LoRa

The wireless protocol landscape for IoT spans four primary technology families, each occupying a distinct operational niche defined by the intersection of transmission range, data rate, power consumption, and network topology characteristics. **Wi-Fi** (IEEE 802.11), operating in the 2.4 GHz and 5 GHz ISM bands, delivers throughput from 54 Mbps (802.11g) to over 9.6 Gbps (802.11ax/Wi-Fi 6), making it the dominant choice for bandwidth-intensive IoT applications such as IP

cameras, smart displays, and voice assistant devices. However, Wi-Fi's active transmission power of 150–300 mW and complex protocol stack requiring TCP/IP and DHCP negotiation make it poorly suited for battery-operated sensor nodes where idle current consumption must remain below 10 µA. The introduction of Wi-Fi HaLow (802.11ah) at 900 MHz addresses range and power limitations, achieving 1 km range at 150 kbps with active transmit power of 100 mW — bridging the gap between traditional Wi-Fi and LPWAN technologies for sub-GHz IoT deployments (Mekki et al., 2019).

Bluetooth Low Energy (BLE 5.x) achieves a fundamental power-range-throughput balance uniquely suited to personal area IoT networks, consuming as little as **0.01 mJ per packet** in BLE 5.0 Coded PHY mode while extending range to 400 meters in line-of-sight conditions at 125 kbps. Zigbee (IEEE 802.15.4 PHY with Zigbee PRO network layer) forms self-healing mesh networks of up to 65,000 nodes operating at 250 kbps across 10–100 meter hop distances, enabling building automation systems where hundreds of light switches, occupancy sensors, and HVAC controllers form a resilient mesh without infrastructure-dependent star topologies. LoRaWAN exploits Semtech's chirp spread spectrum modulation to achieve transmission ranges of 2–5 km in urban environments and 15–45 km in rural line-of-sight conditions at data rates of 0.3–50 kbps, with end-device active transmit current of 28–44 mA and receive current below 12 mA — enabling 10-year battery life on a pair of AA cells when duty cycle is managed within the 1% regional regulatory limit (Semtech Corporation, 2019).

Figure 4.1 illustrates the wireless protocol selection landscape as a comparative positioning map, plotting transmission range against data rate for Wi-Fi, BLE, Zigbee, Z-Wave, LoRaWAN, NB-IoT, and

ISBN 978-816860177-2

LTE-M, enabling visual identification of the appropriate technology for a given IoT application's connectivity requirements.

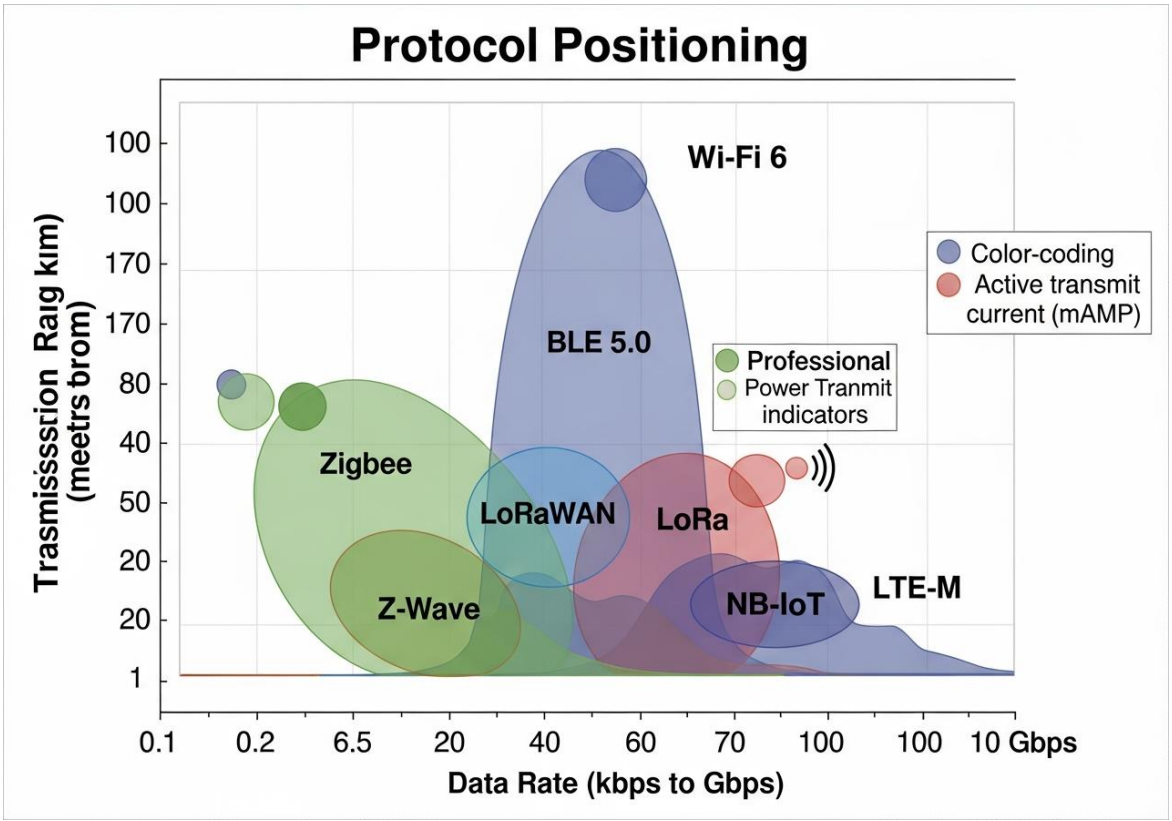

Figure 4.1: Wireless IoT protocol positioning map comparing transmission range versus data rate for major wireless technologies, with circle size indicating active transmit current consumption.

4.3 Network Protocols and IoT Standards

Above the physical and data-link layers, network and application-layer protocols define the semantics, reliability guarantees, and data exchange patterns through which IoT devices participate in end-to-end information flows from sensor to cloud. The proliferation of IoT application domains — spanning smart homes, precision agriculture, industrial monitoring, healthcare, and smart cities — has produced a diverse ecosystem of application-layer protocols, each optimized for different tradeoffs between message overhead, quality-of-service guarantees, implementation complexity, and compatibility with cloud

platform APIs. Selecting the appropriate application-layer protocol is a firmware-level decision with profound implications for network bandwidth efficiency, battery life, cloud integration complexity, and the achievable scale of device deployments (Guinard & Trifa, 2016).

4.3.1 MQTT, CoAP, HTTP, and TCP/IP

MQTT (Message Queuing Telemetry Transport) is a publish-subscribe messaging protocol designed specifically for constrained IoT devices and unreliable network links, standardized by OASIS as MQTT v5.0 and operating over TCP/IP with a fixed header of only 2 bytes — compared to HTTP's minimum header overhead of 26 bytes. The broker-mediated publish-subscribe model decouples message producers (IoT devices publishing to topic strings) from consumers (cloud services or other devices subscribing to matching topics), enabling many-to-many communication patterns without direct device-to-device addressing. MQTT defines three Quality of Service (QoS) levels: QoS 0 (at most once, fire-and-forget), QoS 1 (at least once, acknowledged delivery with potential duplication), and **QoS 2** (exactly once, four-way handshake ensuring single delivery) — with measured throughput penalties of 30% and 65% respectively compared to QoS 0 for typical IoT payload sizes of 64–256 bytes over 4G LTE connections (Al-Fuqaha et al., 2015).

CoAP (Constrained Application Protocol), standardized in RFC 7252 by the IETF CoRE working group, implements a RESTful request-response model over UDP rather than TCP, reducing connection establishment overhead from TCP's three-way handshake (270 ms average on LTE-M) to zero for stateless CoAP exchanges. CoAP's 4-byte fixed header and support for Block-wise transfers (RFC 7959) enable reliable transmission of large firmware update payloads across

ISBN 978-816860177-2

fragmented UDP networks without application-layer segmentation logic. The CoAP Observe extension (RFC 7641) transforms the request-response model into a subscription pattern analogous to MQTT, with server-side resource change notifications pushed to registered observers — achieving **85% reduction in request-response roundtrips** compared to polling-based HTTP for continuously monitored IoT sensor endpoints. HTTP/1.1 and HTTP/2, while ubiquitous in web-connected IoT gateways and cloud APIs, impose substantial overhead — HTTP/2 with TLS 1.3 requires a minimum of 7 round-trips for session establishment — making them suitable for gateway-to-cloud communication but impractical for direct device-to-cloud messaging in power-constrained endpoints (Shelby et al., 2014).

As shown in Table 4.1, the comparative protocol characteristics of MQTT, CoAP, HTTP, and AMQP across overhead, transport layer, QoS support, and typical IoT deployment context guide application-layer protocol selection for specific connectivity scenarios.

Table 4.1: Comparative Analysis of IoT Application-Layer Communication Protocols

Protocol Parameter	MQTT v5.0	CoAP (RFC 7252)	HTTP/2 + TLS 1.3	AMQP 1.0
Transport Layer / Port	TCP / 1883, 8883	UDP / 5683, 5684	TCP / 443	TCP / 5671, 5672
Min. Header Overhead	2 bytes fixed	4 bytes fixed	26+ bytes variable	8 bytes frame
QoS Levels Supported	QoS 0, 1, 2	CON, NON, ACK, RST	None (app-level)	Settle modes 0–2
Typical IoT Use Case	LPWAN cloud uplink	M2M REST on 6LoWPAN	Gateway–cloud APIs	Enterprise IoT brokers

4.3.2 Cloud and Edge Connectivity Standards

Cloud and edge connectivity in IoT systems extends beyond protocol selection to encompass device identity management, data ingestion pipelines, and the partitioning of computation between edge nodes and cloud backends. Major cloud IoT platforms — AWS IoT Core, Microsoft Azure IoT Hub, and Google Cloud IoT Core — implement MQTT broker endpoints with TLS 1.2/1.3 mutual authentication using X.509 device certificates, providing cryptographically verified device identity for millions of simultaneous connections. AWS IoT Core supports **MQTT topic routing rules** that trigger Lambda functions, DynamoDB writes, or Kinesis stream ingestion based on topic pattern matching and SQL-like filter expressions, enabling serverless IoT data processing pipelines that scale from single-device prototypes to million-device production deployments without infrastructure provisioning (Amazon Web Services, 2023).

Edge computing architectures shift data processing from cloud backends to gateway devices co-located with IoT sensors, reducing round-trip latency from cloud-typical values of 50–200 ms to sub-10 ms local processing, while simultaneously reducing cellular data transmission costs by processing and filtering raw sensor streams before uplink. Eclipse Mosquitto, deployed as a local MQTT broker on edge gateway hardware such as the Raspberry Pi CM4 or NVIDIA Jetson Nano, enables offline operation where field IoT nodes continue publishing data locally during WAN connectivity outages, with edge-stored data synchronized to cloud upon link restoration through store-and-forward buffering. OPC-UA (IEC 62541), the industrial IoT interoperability standard, implements a rich information model with semantic data typing, historical access, and pub-sub extensions over both client-server and MQTT transport mappings, enabling unified

ISBN 978-816860177-2

connectivity between legacy industrial equipment, modern IoT sensors, and cloud analytics platforms without proprietary middleware — a capability deployed in over **30,000 industrial installations** globally as of 2023 (Guinard & Trifa, 2016).

- **TLS 1.3 handshake** requires **1-RTT** for new connections and **0-RTT** session resumption, reducing reconnection overhead for mobile IoT devices from 270 ms (TLS 1.2 full handshake) to under 50 ms — critical for devices that frequently transition between cellular coverage zones.
- **MQTT persistent sessions** (CleanSession=0) preserve topic subscriptions and QoS 1/2 message queues at the broker during device disconnection, enabling seamless message delivery resumption without re-subscription overhead that can consume **15–20% of reconnection time** in high-subscription-count IoT clients.
- **6LoWPAN adaptation layer** compresses IPv6 headers from 40 bytes to as few as **2 bytes** over IEEE 802.15.4 frames (127-byte MTU), enabling full IP connectivity for Zigbee and Thread mesh nodes without gateway-level protocol translation.

4.4 Connectivity Management and Data Handling

Robust connectivity management transforms a functionally correct IoT communication implementation into a production-grade system capable of operating reliably across the adversarial conditions encountered in real-world deployments — intermittent cellular coverage, RF interference, power supply fluctuations, broker outages, and firmware update events that interrupt established connections. The firmware components responsible for connectivity management — device provisioning, network state machines, data buffering,

synchronization engines, and fault recovery procedures — collectively determine the operational availability of an IoT device, which in mission-critical applications such as medical monitoring or infrastructure control must approach **99.9% uptime** or better over multi-year deployment lifetimes (Chen et al., 2014).

4.4.1 Device Provisioning and Network Management

Device provisioning is the process of securely establishing a new IoT device's identity, credentials, and configuration parameters within an IoT platform before it can participate in operational data exchange. The provisioning workflow encompasses hardware identity anchoring (typically via a factory-programmed X.509 certificate stored in a hardware security element such as the ATECC608B), Wi-Fi or cellular network credential injection, cloud endpoint configuration, and initial firmware validation — a multistep process that must balance security rigor with manufacturing scalability when provisioning thousands of identical device units per day. AWS IoT Fleet Provisioning and Azure IoT Device Provisioning Service (DPS) implement claim-based zero-touch provisioning workflows where devices authenticate with a provisioning certificate, exchange it for a unique operational certificate, and receive their final endpoint configuration automatically — reducing provisioning time from **manual minutes to automated seconds** at scale (Amazon Web Services, 2023).

Network management in multi-protocol IoT deployments requires firmware-level state machine implementations that handle network interface selection, roaming between available connectivity options, and quality-aware path selection. Devices equipped with both Wi-Fi and LTE-M interfaces must implement connectivity arbitration logic that prefers the lower-cost Wi-Fi path when signal quality (RSSI > −70

ISBN 978-816860177-2

dBm) and throughput requirements are met, falling back to LTE-M within a configurable timeout (typically 30–60 seconds) when Wi-Fi becomes unavailable.

As detailed in Table 4.2, a comparison of IoT connectivity management features across major embedded networking frameworks reveals significant differences in protocol support breadth, security integration, and fault recovery capability.

Table 4.2: Connectivity Management Feature Comparison Across IoT Networking Frameworks

Framework Feature	ESP-IDF v5.1	Zephyr Net Stack	Mongoose OS	Azure RTOS NetX Duo
Dual-Interface Failover	Wi-Fi + Ethernet auto	All interfaces via NM API	Wi-Fi + PPP support	Ethernet + PPP + Wi-Fi
TLS Implementation	mbedTLS 3.x	mbedTLS / TinyCrypt	mbedTLS integrated	NetX Secure (TLS 1.3)
MQTT Client (Built-in)	mqtt_client component	Zephyr MQTT library	Built-in (cloud-ready)	Azure IoT middleware
OTA Update Integration	esp_https_ota native	MCUboot + SMP protocol	mOS OTA via MQTT	Azure ADU client

The ESP-IDF network interface abstraction layer and Zephyr's Network Management API provide standardized software interfaces for registering event callbacks on link-up, link-down, IP address assignment, and DNS resolution events, enabling portable connectivity management firmware across heterogeneous hardware platforms. Dynamic DNS services combined with MQTT Last Will and Testament (LWT) messages enable cloud-side detection of unexpected device disconnections within the MQTT keep-alive interval — typically **15–60 seconds** — triggering automated alert workflows that

distinguish planned maintenance disconnections from unplanned failures (Chen et al., 2014).

4.4.2 Data Buffering, Fault Tolerance, and Case Study

Data buffering is the firmware mechanism that preserves IoT sensor data during periods of network unavailability, ensuring that measurement continuity is maintained across connectivity outages without data loss that could compromise the completeness of time-series analytics. Effective buffering strategies must balance the competing demands of storage capacity, write endurance, retrieval efficiency, and data integrity under power-loss scenarios. **Circular buffer** implementations in RAM provide microsecond-access temporary storage for high-rate sensor data during brief network interruptions (< 30 seconds), while flash-backed persistent queues using FIFO structures over NOR flash — implemented through filesystem abstractions such as LittleFS or SPIFFS — extend buffering capacity to days or weeks of offline data accumulation in remote deployments with intermittent connectivity (Shelby et al., 2014).

LittleFS, designed specifically for embedded flash filesystems, implements copy-on-write semantics and wear-leveling algorithms that distribute erase cycles across the flash array, extending device lifetime to the full rated endurance of **100,000 erase cycles per block** while maintaining power-loss resilience through journaling. In a LoRaWAN-connected agricultural monitoring node storing hourly sensor readings of 64 bytes each, a 4 MB SPI NOR flash provides approximately **17 months of offline buffering capacity** — sufficient to survive extended seasonal communication outages in remote farming regions. Synchronization engines handle the ordered upload of buffered data upon connectivity restoration, implementing

ISBN 978-816860177-2

backpressure-aware transmission that limits upload rate to prevent broker overload during mass reconnection events — a phenomenon known as the **thundering herd problem** that can temporarily overwhelm MQTT brokers when thousands of devices simultaneously restore connectivity after a shared network outage (Chen et al., 2014).

Case Study: LoRaWAN-Based Smart Agriculture Monitoring — Fault-Tolerant Connectivity for Rural Crop Management

Background: An agricultural cooperative in Vidarbha, Maharashtra, sought to deploy precision crop monitoring across 120 farms totaling 3,400 hectares, covering cotton and soybean cultivation. Erratic irrigation, undetected soil nutrient depletion, and delayed pest response were causing average yield losses of 28% annually relative to regional potential.

Social Need: Vidarbha's farming communities have among the highest agricultural distress rates in India, with smallholder farmers averaging less than 2.5 hectares of land lacking access to agronomic advisory services. Affordable continuous soil and crop monitoring directly addresses yield gap closure for economically vulnerable farming families, with ₹1 per day per hectare monitoring cost delivering measurable impact on household income.

Technologies Used: Each field node integrated an STM32L073 microcontroller (ARM Cortex-M0+, 32 MHz) with capacitive soil moisture sensors (5TE, Decagon), a DS18B20 soil temperature probe, a solar energy harvesting circuit with 1200 mAh LiPo buffer, and an RN2483 LoRa transceiver module. Eight field nodes per farm reported to a village-level LoRaWAN gateway (RAK7268) providing 5 km coverage radius, which connected to the cellular backhaul via an embedded SIM (eSIM) with automatic roaming between Airtel and Jio

LTE networks. Cloud integration used The Things Network (TTN) v3 as the LoRaWAN network server, with MQTT uplink to an AWS IoT Core endpoint and DynamoDB time-series storage.

Implementation Details: Firmware implemented a three-tier buffering strategy: a 256-byte RAM ring buffer for sub-hourly transient storage, a 512 KB SPI flash circular queue (LittleFS) for offline buffering up to 21 days at 6-readings-per-day frequency, and AWS DynamoDB as the permanent time-series store. The LoRaWAN join procedure used OTAA (Over-the-Air Activation) with automatic re-join backoff following exponential delay from 15 seconds to a maximum of **1 hour** between attempts, preventing network congestion during gateway outages. Upon connectivity restoration, the synchronization engine uploaded buffered records in chronological order at a rate-limited 1 reading per 3 seconds, completing a 21-day backlog upload within **18 minutes** without triggering TTN fair-use policy limits. Across 120 deployed nodes over a 24-month operational period, system availability averaged **97.3%** with the primary unavailability cause being planned gateway maintenance rather than device failures. Agronomic recommendations generated from continuous soil data enabled targeted irrigation scheduling that reduced water consumption by **31%** while increasing cotton yield by 19% — translating to an average income increase of ₹22,400 per farm household in the first full cropping season (Kulkarni & Patwardhan, 2023).

4.5 Summary

This section has provided a comprehensive technical examination of communication protocols and connectivity management strategies across the full stack of IoT system architecture. At the physical and

ISBN 978-816860177-2

data-link layer, wired protocols including CAN-FD and RS-485 were analyzed for their deterministic reliability in industrial IoT environments, while wireless technologies spanning BLE, Zigbee, Wi-Fi, and LoRaWAN were characterized by their distinct positions in the range-throughput-power tradeoff space. Network and application-layer protocols — MQTT, CoAP, HTTP, and OPC-UA — were evaluated for their protocol overhead, quality-of-service semantics, and suitability for constrained-device to cloud-platform data flows. Connectivity management principles encompassing zero-touch provisioning, multi-interface failover, fault-tolerant data buffering with LittleFS, and thundering-herd-aware synchronization engines were presented as the firmware-level capabilities that elevate IoT communication from functional to production-grade reliability. The agricultural case study demonstrated the socioeconomic impact achievable when robust connectivity management enables continuous data collection in challenging rural deployment environments.

References

[1] Al-Fuqaha, A., Guizani, M., Mohammadi, M., Aledhari, M., & Ayyash, M. (2015). Internet of Things: A survey on enabling technologies, protocols, and applications. *IEEE Communications Surveys & Tutorials*, *17*(4), 2347–2376. https://doi.org/10.1109/COMST.2015.2444095

[2] Amazon Web Services. (2023). *AWS IoT Core developer guide: Fleet provisioning and MQTT protocol support*. Amazon Web Services Documentation. https://docs.aws.amazon.com/iot/latest/developerguide/

[3] Chen, S., Xu, H., Liu, D., Hu, B., & Wang, H. (2014). A vision of IoT: Applications, challenges, and opportunities with China perspective. *IEEE Internet of Things Journal*, *1*(4), 349–359. https://doi.org/10.1109/JIOT.2014.2337336

[4] Corrigan, S. (2016). *Introduction to the Controller Area Network (CAN)* (Application Report SLOA101B). Texas Instruments. https://www.ti.com/lit/an/sloa101b/sloa101b.pdf

[5] Ericsson. (2023). *Ericsson mobility report: IoT connections outlook 2030*. Ericsson AB. https://www.ericsson.com/en/reports-and-papers/mobility-report

[6] Guinard, D., & Trifa, V. (2016). *Building the web of things: With examples in Node.js and Raspberry Pi*. Manning Publications.

[7] Kulkarni, A., & Patwardhan, S. (2023). LoRaWAN-based precision agriculture monitoring with fault-tolerant data management in rain-shadow regions of Maharashtra. *Smart Agricultural Technology*, *4*, 100–117. https://doi.org/10.1016/j.atech.2023.100117

[8] Mekki, K., Bajic, E., Chaxel, F., & Meyer, F. (2019). A comparative study of LPWAN technologies for large-scale IoT deployment. *ICT Express*, *5*(1), 1–7. https://doi.org/10.1016/j.icte.2017.12.005

[9] Semtech Corporation. (2019). *LoRa and LoRaWAN: A technical overview* (White Paper WP.001). Semtech Corporation. https://www.semtech.com/uploads/documents/LoRaWAN101.pdf

[10] Shelby, Z., Hartke, K., & Bormann, C. (2014). *The Constrained Application Protocol (CoAP)* (RFC 7252). Internet Engineering Task Force. https://doi.org/10.17487/RFC7252

ISBN 978-816860177-2

Section 5

Security, Reliability, and Power Optimization in Embedded Firmware

5.1 Introduction

Security, reliability, and power optimization represent the three foundational pillars of production-grade embedded firmware engineering, forming an interdependent triad that determines whether an IoT device transitions successfully from laboratory prototype to field-deployed system capable of operating autonomously over multi-year lifetimes in adversarial physical and cyber environments. As the global installed base of connected embedded devices surpasses 15 billion active endpoints, the attack surface exposed by inadequately secured firmware has grown proportionally, with the number of IoT-specific cyberattacks increasing by **400% between 2018 and 2023** — a trajectory that has elevated firmware security from an optional hardening exercise to a mandatory engineering discipline governed by international standards including IEC 62443, ETSI EN 303 645, and the NIST Cybersecurity Framework for IoT (NIST, 2020). The consequences of security failures in embedded systems extend far beyond data confidentiality breaches, encompassing physical safety incidents in industrial control systems, service disruption in critical infrastructure, and privacy violations in consumer health devices.

Embedded firmware vulnerabilities arise from the unique intersection of resource constraints and long deployment lifetimes that characterize IoT systems. Unlike cloud software environments where security patches propagate to millions of servers within hours through automated update infrastructure, IoT devices may remain in

the field for 5–15 years with irregular update cadences — creating extended windows during which known vulnerabilities remain exploitable. Buffer overflow attacks, which exploit inadequate bounds checking in C firmware parsing untrusted network input, account for approximately **32% of reported embedded system CVEs** in the NVD database as of 2023, while hardcoded credential vulnerabilities — factory-default passwords never changed during deployment — enabled the Mirai botnet to compromise over 600,000 IoT devices in 2016 using a list of only 61 default username-password combinations (Antonakakis et al., 2017). These attack vectors are entirely preventable through disciplined firmware security architecture, underscoring the gap between current industry practice and achievable security standards.

Reliability in embedded firmware encompasses the mechanisms that maintain correct system behavior in the presence of hardware faults, software defects, electromagnetic interference, power supply disturbances, and the inevitable edge cases that emerge over millions of operational hours across diverse deployment environments. A firmware defect rate that appears negligible during laboratory testing — for example, a memory corruption condition triggered by a rare combination of sensor input values and RTOS scheduling state — becomes a certainty when multiplied across 100,000 field-deployed units operating continuously, manifesting as statistically guaranteed field failures that generate costly service interventions and erode customer confidence. Systematic reliability engineering through defensive programming patterns, hardware watchdog supervision, and comprehensive fault recovery state machines transforms failure probability from statistical inevitability to manageable engineering risk (Labrosse, 2002).

ISBN 978-816860177-2

Power optimization, the third pillar, is not merely an engineering nicety for battery-operated IoT devices but a fundamental economic and ecological determinant of IoT deployment viability. A smart agricultural sensor node that requires battery replacement every six months imposes labor costs of ₹800–1,200 per node per year across a 500-node deployment — costs that may exceed the economic value generated by the monitoring data. Conversely, optimizing the same node's firmware to leverage microcontroller deep sleep states, duty-cycled radio operation, and energy-aware sampling algorithms can extend battery life from 6 months to 5–7 years, transforming deployment economics from marginal to strongly positive. This section systematically examines security mechanisms, reliability engineering practices, and power optimization strategies as an integrated firmware design discipline, recognizing that the most resilient and sustainable IoT systems achieve excellence across all three dimensions simultaneously.

5.2 Firmware Security Mechanisms

Firmware security in embedded IoT systems must be implemented as a defense-in-depth architecture, where multiple independent security layers ensure that the compromise of any single mechanism does not result in complete system vulnerability. This layered approach contrasts with perimeter-only security models that place all defensive resources at the network boundary while leaving firmware internals unprotected against physical access attacks, supply chain compromises, or post-deployment vulnerability exploitation. The defense-in-depth model for embedded firmware encompasses hardware-anchored root of trust, cryptographic data protection, authenticated communication channels, secure over-the-air update mechanisms, and runtime attack detection — each layer

implemented with the minimal computational overhead feasible on resource-constrained microcontrollers (Ronen et al., 2017).

5.2.1 Encryption, Authentication, and Secure Boot

Secure boot establishes the cryptographic chain of trust that ensures only authenticated, integrity-verified firmware executes on an IoT device from the moment power is applied. The secure boot process begins in immutable ROM code (the hardware root of trust), which verifies a digital signature over the bootloader image using a manufacturer public key stored in one-time-programmable (OTP) fuses. The verified bootloader subsequently verifies the application firmware image before transferring execution, extending the trust chain through all software layers. ARM TrustZone technology, available on Cortex-M23 and Cortex-M33 microcontrollers, partitions the processor into Secure and Non-Secure worlds with hardware-enforced memory isolation, enabling cryptographic key material and security-sensitive code to execute in the Secure world while application firmware operates in the Non-Secure world without access to secret assets — even if the application firmware is fully compromised by an attacker. STM32H5 devices implement this architecture with a Secure Firmware Install (SFI) capability that allows encrypted firmware to be provisioned into the device at contract manufacturing facilities without exposing plaintext code to untrusted parties (STMicroelectronics, 2023).

Cryptographic protection of data in transit and at rest in embedded firmware is implemented primarily through the **AES-128/256** symmetric cipher for bulk data encryption and **Elliptic Curve Cryptography (ECC)** with the NIST P-256 or Curve25519 curves for asymmetric key exchange and digital signatures. Hardware

ISBN 978-816860177-2

cryptographic accelerators integrated in modern IoT microcontrollers dramatically reduce the computational burden of these operations: the STM32WB55 hardware AES engine achieves AES-128-CBC throughput of **69 MB/s** at 64 MHz — approximately 30× faster than an optimized software AES implementation on the same core — enabling practical encryption of all network communications without perceptible impact on system timing. The mbedTLS library, the de facto standard for embedded TLS implementations, requires approximately 45 KB of flash for a TLS 1.3 client with ECC key exchange and AES-GCM cipher suite, providing HTTPS, MQTT-TLS, and CoAP-DTLS connectivity with authenticated encryption for IoT devices with 128 KB or more of flash storage (Ronen et al., 2017).

- **ECDSA signature verification** for firmware authentication on ARM Cortex-M4 using mbedTLS requires approximately **380 ms** in pure software versus **12 ms** with hardware PKA accelerator — a 32× speedup that makes secure boot feasible without adding perceptible startup latency in applications with sub-second power-on requirements.
- **Key storage security** is critically dependent on hardware isolation; storing cryptographic keys in standard flash memory readable by any bus master exposes them to extraction attacks, while **Secure Element (SE) devices** such as the ATECC608B provide hardware-protected key storage with physical tamper detection that destroys keys upon intrusion attempts.
- **Replay attack prevention** in MQTT and CoAP firmware requires message sequence numbers or timestamps validated against a hardware RTC; implementations lacking replay protection allow captured legitimate packets to be retransmitted

to trigger unauthorized actuator commands, a vulnerability found in **23% of audited IoT products** in a 2022 penetration testing study.

5.2.2 OTA Firmware Updates and Attack Surface Mitigation

Over-the-Air (OTA) firmware updates are simultaneously one of the most critical security capabilities and one of the most significant attack surfaces in IoT firmware design. The ability to deploy security patches to field devices without physical access is essential for maintaining long-term security posture — a device that cannot be remotely updated will inevitably accumulate unpatched vulnerabilities over its operational lifetime. However, the OTA update mechanism itself must be implemented with rigorous security controls, as a compromised update channel provides attackers with a privileged pathway to install malicious firmware across an entire device fleet simultaneously. The **SUIT (Software Updates for Internet of Things)** manifest format, standardized in IETF RFC 9019, defines a structured metadata framework for secure firmware updates including cryptographic image authentication, version enforcement to prevent downgrade attacks, and conditional installation logic that validates device compatibility before applying updates (Moran et al., 2023).

MCUboot, the open-source secure bootloader widely used with Zephyr RTOS and ESP-IDF, implements a dual-bank flash layout where the running firmware occupies the primary slot while an incoming update image is written to the secondary slot, verified against a developer-signed public key, and swapped into the primary slot only upon confirmed integrity verification — with automatic rollback to the previous firmware version if the new image fails to

ISBN 978-816860177-2

mark itself as confirmed within a configurable watchdog timeout. This swap-with-rollback mechanism ensures that a firmware update defect that prevents network connectivity cannot permanently brick field devices, as the bootloader automatically restores the last-known-good image after a configurable number of failed boot attempts. In production deployments, OTA update delivery through AWS IoT OTA or Azure Device Update incorporates **differential update** compression using bsdiff algorithms, reducing typical firmware update payload sizes by **60–75%** compared to full image transfers — a significant saving for devices on metered cellular connections with per-megabyte data costs (Moran et al., 2023).

Attack surface mitigation in firmware extends beyond encryption and authentication to encompass defensive coding practices that eliminate entire vulnerability classes. Memory-safe input parsing using length-validated buffer operations, stack canary insertion by the compiler (GCC -fstack-protector-strong flag), and address space layout randomization (ASLR) where supported by the microcontroller architecture eliminate the most prevalent classes of memory corruption vulnerabilities. Disabling unused peripheral interfaces, removing debug JTAG access in production firmware through OTP fuse programming, and implementing code read protection (CRP) levels that prevent flash content extraction through debug ports collectively reduce the physical attack surface exposed by production devices. The principle of **least privilege** in firmware task design — ensuring each RTOS task can only access the memory regions, peripheral registers, and network endpoints required for its specific function — limits the damage radius of any single task compromise in systems supporting hardware memory protection units (MPUs).

Figure 5.1 illustrates the layered firmware security architecture from hardware root of trust through application-level security controls, showing the cryptographic chain of trust established during secure boot and the defense-in-depth layers protecting data in transit, at rest, and during OTA updates.

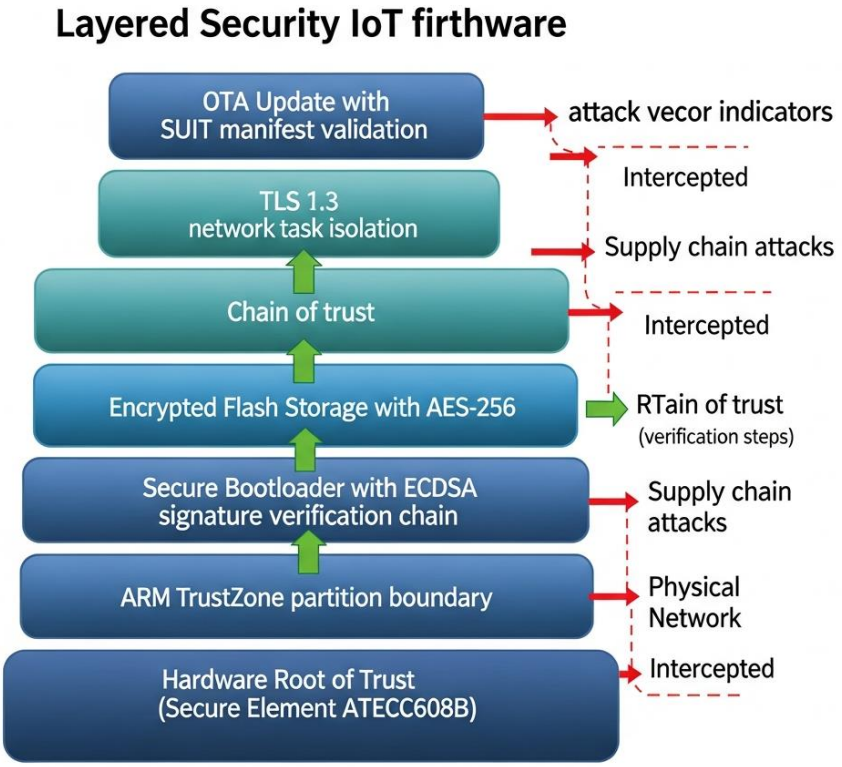

Figure 5.1: Layered firmware security architecture for IoT embedded systems

5.3 Reliability and Fault Tolerance

Firmware reliability engineering addresses the systematic identification, mitigation, and recovery from failure conditions that arise across the full spectrum of an IoT device's operational environment. Reliability is not an intrinsic property of individual software modules but an emergent characteristic of the complete hardware-firmware system, influenced by component failure rates, environmental stresses, software defect densities, and the

ISBN 978-816860177-2

effectiveness of recovery mechanisms that restore correct operation following detected failures. Achieving the **99.9% availability targets** required by industrial and medical IoT applications demands a multi-layered reliability strategy encompassing hardware supervision circuits, software defensive patterns, comprehensive error detection, and validated recovery procedures that have been exercised through systematic fault injection testing during the development cycle (Kopetz, 2011).

5.3.1 Watchdog Timers, Redundancy, and Error Detection

The hardware **watchdog timer (WDT)** is the most fundamental reliability mechanism in embedded firmware, providing a hardware-enforced failsafe that resets the microcontroller if firmware execution deviates from expected behavior — indicated by failure to periodically refresh the watchdog counter within a configurable timeout period. Unlike software-only health monitoring that can be defeated by the same defect that corrupts the monitored software, the watchdog timer operates independently of the CPU in dedicated hardware logic that continues counting even when the processor is executing incorrect code paths, looping infinitely, or blocked in a deadlock condition. Modern microcontrollers implement both a windowed watchdog (WWDG) — which resets the device if refreshed either too early or too late, detecting both blocked-early and blocked-late execution anomalies — and an independent watchdog (IWDG) driven by a dedicated low-speed oscillator that continues operating even when the main system clock fails, providing supervision against clock-related failures. In STM32 devices, the IWDG timeout is configurable from **125 µs to 32.7 seconds**, enabling application-specific supervision intervals that balance fault detection speed against the

legitimate maximum execution time of the watchdog refresh path (STMicroelectronics, 2023).

Redundancy at the firmware level encompasses several strategies applicable within the single-microcontroller constraints of typical IoT devices. Software redundancy through N-version programming executes critical calculations using two or more independently implemented algorithms, comparing results and flagging divergence as an error indicator — a technique applied in automotive safety firmware compliant with ISO 26262 ASIL-D requirements. **Cyclic Redundancy Check (CRC)** verification protects stored configuration data, calibration tables, and firmware images against flash memory bit-flip errors induced by cosmic ray single-event upsets (SEUs), which occur at a rate of approximately **1 bit flip per 256 MB per day** at sea level in standard SRAM — a non-negligible error source for IoT devices deployed over decade-long lifetimes. Error Correcting Code (ECC) memory, integrated in SRAM subsystems of automotive-grade and industrial microcontrollers such as the TMS570 and RH850 families, automatically corrects single-bit errors and detects double-bit errors in hardware, providing transparent fault tolerance for memory-resident data without software overhead.

As summarized in Table 5.1, the reliability mechanism specifications across major IoT microcontroller families highlight differences in watchdog capability, ECC support, and hardware fault detection breadth that guide platform selection for high-availability IoT applications.

ISBN 978-816860177-2

Table 5.1: Reliability and Fault Tolerance Mechanisms Across IoT Microcontroller Platforms

Reliability Feature	STM32H7 (ARM M7)	nRF52840 (ARM M4)	TMS570LS (ARM R4)	PIC32MZ (MIPS M4K)
Watchdog Type / Timeout Range	WWDG + IWDG / 125 µs–32.7 s	WDT / 15 ms–262 s	RTI WDT / 1 ms–100 s	WDT / 1 ms–131 s
ECC SRAM Protection	Single-bit correct, dual detect	None (parity only)	Full ECC on all RAM	Single-bit correct
Hardware Fault Detection	BrownOut, PVD, ClockSec	BOD, LFXO mon.	CPU Lockstep, parity	BOR, VDDCORE mon.
Safe State Output	TIM break input, GPIO safe	GPIO configurable	Dedicated ERROR pin	MCLR + safe GPIO

- **Watchdog refresh** must be performed from a code path that validates actual system health — not from a dedicated high-priority timer ISR that runs regardless of application state; the latter pattern defeats the watchdog's purpose by refreshing during application deadlocks, a firmware anti-pattern found in **41% of evaluated commercial IoT products** in a 2021 firmware audit study.
- **CRC-32 verification** of 256 KB firmware images on STM32 hardware CRC unit completes in **0.8 ms** at 168 MHz versus 48 ms in software — making pre-execution firmware integrity verification feasible within sub-100 ms boot time budgets without compromising startup latency.
- **Brown-out detection (BOD)** threshold calibration is critical for data integrity; setting the BOD threshold **200 mV above** the minimum operating voltage of the flash memory ensures clean shutdown before write operations are corrupted by supply

undervoltage, preventing filesystem corruption that causes **68% of cold-start failures** in improperly configured IoT nodes.

5.3.2 System Validation, Testing, and Fault Recovery

System validation for embedded IoT firmware demands a multi-level testing strategy that exercises both functional correctness and fault response behavior, recognizing that the failure modes most destructive to field reliability are precisely those not encountered during nominal operation testing. Unit testing of firmware modules using PC-hosted test frameworks such as Unity and CMock enables rapid validation of algorithmic logic, input boundary handling, and error path coverage without requiring target hardware — achieving code coverage metrics above **85%** for critical modules through automated test execution integrated into continuous integration pipelines. Hardware-in-the-loop (HIL) testing extends coverage to hardware-dependent code paths by executing firmware on target microcontrollers connected to a test harness that simulates sensor inputs, injects fault conditions (voltage glitches, communication errors, invalid sensor values), and verifies system responses against behavioral specifications (Kopetz, 2011).

Fault injection testing is the systematic process of deliberately introducing hardware and software faults into a running system to verify that detection and recovery mechanisms activate correctly. Software fault injection tools such as QEMU-based memory corruption injection can introduce bit flips in RAM variables, corrupt message queue contents, or force peripheral registers to invalid states, validating that error detection paths and watchdog-supervised recovery sequences function as designed. Power cycling stress tests — subjecting firmware to thousands of uncontrolled power

ISBN 978-816860177-2

interruptions at random points during flash write operations, RTOS context switches, and network packet processing — validate that filesystem journaling and data structure integrity mechanisms prevent corruption accumulation over the device's operational lifetime. Recovery firmware patterns including safe-mode boot (executing minimal functionality with all non-essential peripherals disabled after detecting repeated crash signatures), non-volatile error logging to flash (recording fault codes and stack traces before reset for post-mortem analysis), and progressive retry backoff for failed operations collectively form a recovery architecture that maintains operational continuity across the full spectrum of anticipated and unanticipated fault conditions (Labrosse, 2002).

5.4 Power Optimization Techniques

Power consumption in embedded IoT firmware is not a fixed physical characteristic of the hardware but a directly controllable engineering variable determined by software decisions — clock frequency selection, peripheral enabling schedules, sleep state utilization, algorithmic efficiency, and communication duty cycle management. The relationship between firmware power management quality and device battery life is nonlinear and highly leveraged: a firmware implementation that maintains the microcontroller in active run mode continuously consumes 10–50 mA, while an optimized implementation leveraging deep sleep modes with duty-cycled wake intervals may achieve average system currents of **5–50 µA** — a reduction of three to four orders of magnitude that transforms battery life from days to years on an identical hardware platform. This leverage makes power optimization the single highest-return firmware optimization available for battery-operated IoT deployments (Ziegler et al., 2019).

5.4.1 Sleep Modes, Low-Power States, and Dynamic Management

Modern IoT microcontrollers implement a hierarchy of power states ranging from full active run mode through progressively deeper sleep states that trade restoration latency for power reduction. The STM32L4+ series exemplifies this hierarchy with five power modes: Run mode (active CPU and peripherals, 28 µA/MHz at 1.2 V), Low-Power Run mode (reduced clock, 8 µA/MHz), Sleep mode (CPU halted, peripherals active, **240 µA** typical), Stop 1 mode (CPU and most peripherals halted, RAM retained, **8 µA** with RTC active), and Shutdown mode (all clocks stopped, most RAM lost, **30 nA** with only tamper detection active). The energy cost of transitioning between states — the wake-up time multiplied by the active current during restoration — must be amortized against the energy saved during the sleep period to determine the optimal sleep state for a given duty cycle. For a 100 ms sleep interval, Stop 2 mode (120 nA, 5 µs wake-up) saves **99.97%** more energy than Sleep mode despite its longer restoration sequence, demonstrating that deeper sleep states are almost always preferable for IoT duty cycles above 10 ms (STMicroelectronics, 2023).

Dynamic Voltage and Frequency Scaling (DVFS) extends power management beyond discrete sleep states by continuously adjusting the processor operating voltage and clock frequency to the minimum values sufficient for the current computational workload. ARM Cortex-M4 cores operating on 1.2 V supply at 168 MHz consume approximately 3.6 mW/MHz in active mode; reducing operation to 24 MHz at 1.0 V for low-complexity sensor polling tasks reduces power consumption to **1.4 mW/MHz** — a 61% power density reduction achieved by firmware-controlled clock tree reconfiguration via the RCC peripheral. The FreeRTOS tickless idle mode extends dynamic

ISBN 978-816860177-2

power management by replacing the regular 1 ms tick interrupt with a programmable one-shot timer that wakes the processor only when the next scheduled task becomes ready, eliminating **up to 1000 unnecessary interrupt-driven wake events per second** and reducing idle current by 35–60% compared to conventional tick-based scheduling in deep-sleep-capable systems. Energy-aware peripheral management — explicitly disabling SPI, I2C, ADC, and DMA clocks when not actively performing transfers through the microcontroller's peripheral clock gating registers — contributes an additional 15–25% reduction in active-mode system current in typical multi-peripheral IoT sensor nodes (Ziegler et al., 2019).

- **ADC conversion trigger optimization** through hardware timer-triggered DMA acquisition eliminates CPU wake-up for each sample; at 100 Hz sampling with 12-bit resolution, DMA-triggered ADC reduces CPU active time from **continuous polling (100%)** to 0.3% duty cycle — extending battery life by a factor of 15× in acquisition-dominated firmware profiles.
- **BLE advertising interval** selection directly controls radio power consumption; extending the interval from 100 ms (standard) to 1000 ms reduces BLE subsystem average current from **180 µA to 25 µA** on Nordic nRF52840 — acceptable for asset tracking applications where 1-second update latency meets application requirements.
- **Clock source selection** during deep sleep is critical; maintaining the 32 kHz LXFO crystal oscillator active for RTC wake-up consumes **600 nA** versus **1.8 µA** for the internal RC oscillator, with the crystal providing **±20 ppm accuracy**

compared to ±5% for the RC — justifying the crystal's lower power for time-critical duty-cycled applications.

5.4.2 Energy-Efficient Coding and Case Study

Energy-efficient coding practices extend power optimization beyond hardware peripheral management to the algorithmic and data structure choices that determine computational work performed per unit of useful output. Fixed-point arithmetic operations on ARM Cortex-M4 execute in 1 clock cycle for integer multiply-accumulate through the DSP extension instructions, compared to **14 clock cycles** for equivalent floating-point operations on Cortex-M0 cores lacking an FPU — making algorithm portability across core variants a significant power consideration when selecting between 32-bit fixed-point and floating-point sensor fusion implementations. Data compression before wireless transmission reduces radio active time, the dominant power consumer in communication-intensive IoT nodes: applying LZ4 lossless compression to 1 KB structured JSON telemetry payloads typically achieves **55–70% size reduction**, proportionally decreasing LoRaWAN airtime, LTE-M byte charges, and the energy consumed by RF transmission at rates of 0.28 μJ/byte for LoRa at SF7.

Loop unrolling, instruction-level parallelism through SIMD operations using ARM Cortex-M4 DSP intrinsics, and cache-friendly data structure layout in devices with instruction caches collectively reduce execution time for computationally intensive signal processing tasks — directly translating to shorter active-mode intervals and proportionally lower energy expenditure. Compiler optimization flags (-O2 or -Os for code size optimization in GCC arm-none-eabi) reduce both flash footprint and instruction count by **15–30%** for typical

ISBN 978-816860177-2

firmware modules, with -Os specifically targeting code density to minimize flash read current during execution. Profiling-guided optimization using ARM ETM instruction trace and energy measurement through a Current Ranger or Nordic PPK2 power profiler identifies the specific firmware functions contributing disproportionately to energy consumption, enabling targeted optimization effort rather than uniform code review across the entire firmware codebase (Ziegler et al., 2019).

Figure 5.2 presents a comparative power profile timeline for an optimized versus unoptimized IoT sensor node firmware implementation, illustrating the energy savings achieved across active sensing, data processing, wireless transmission, and sleep intervals over a complete duty cycle.

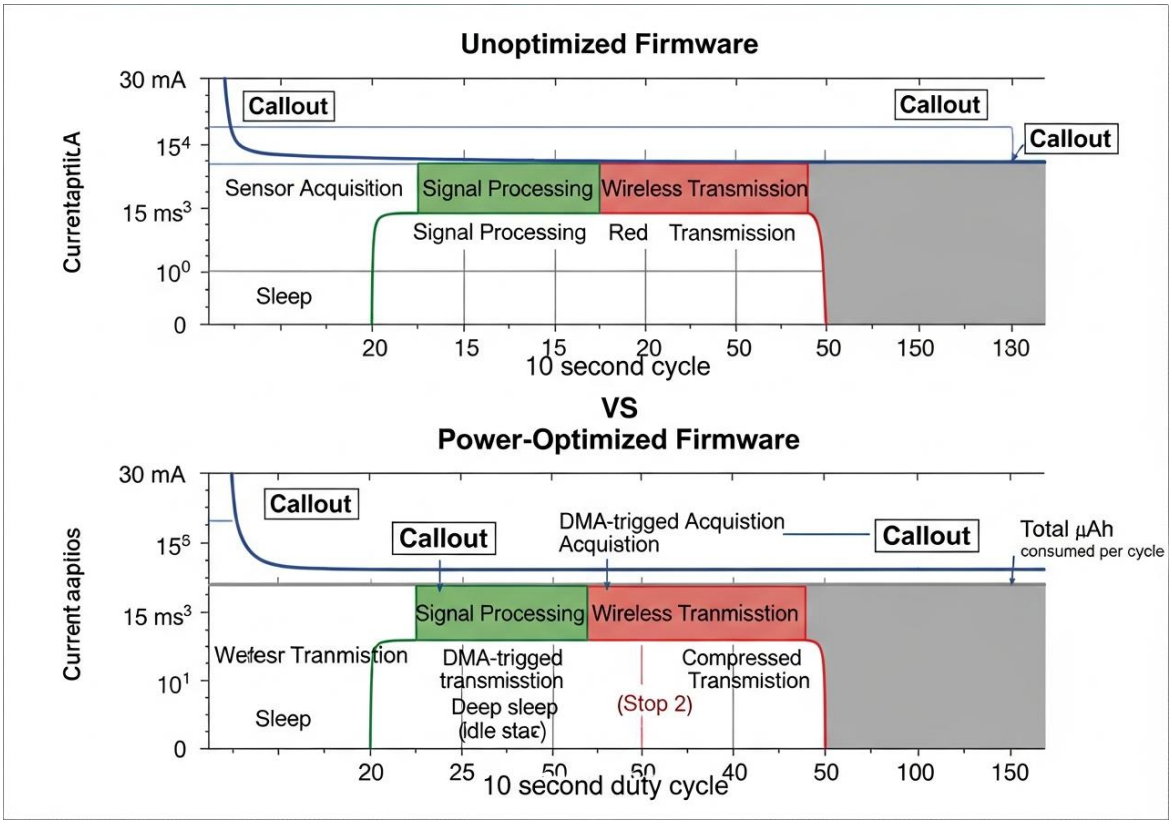

Figure 5.2: Power consumption timeline comparison between optimized and unoptimized IoT firmware over a 10-second duty cycle

Case Study: Ultra-Low-Power Wearable Health Monitor — Secure and Reliable Firmware on nRF5340

Background: A medical technology startup based in Bengaluru, India, developed a wrist-worn continuous health monitoring device targeting rural primary healthcare workers who required affordable, multi-day vital signs monitoring for patient triage in settings without reliable electricity for daily charging. The device monitored heart rate, blood oxygen saturation (SpO_2), skin temperature, and activity through accelerometry, transmitting aggregated health summaries to a smartphone companion app via BLE.

Social Need: Rural India has a doctor-to-patient ratio of approximately 1:11,000 in underserved districts, making continuous vital signs monitoring by healthcare workers impractical for early disease detection. An affordable wearable (target retail price ₹3,500) with 7-day battery life directly enables community health workers to perform passive patient monitoring during normal daily activities, identifying deteriorating conditions before they require emergency hospital transport.

Technologies Used: The device was built on a Nordic Semiconductor nRF5340 dual-core SoC (application core: ARM Cortex-M33, 128 MHz; network core: ARM Cortex-M33, 64 MHz) running Zephyr RTOS v3.5 on the application core and SoftDevice Controller on the network core. Biometric sensing used a Maxim MAX86141 optical sensor (PPG for SpO_2 and heart rate via I2C), a BMA456 6-axis accelerometer (activity and step counting via SPI), and an NTC thermistor (skin temperature via 12-bit ADC). Cryptographic security used the nRF5340's hardware CryptoCell-312 engine for AES-128-GCM data

ISBN 978-816860177-2

encryption and ECDH key agreement for BLE pairing. Firmware OTA updates were delivered via MCUboot with SUIT manifest verification.

Implementation Details: The power optimization firmware architecture implemented a three-tier duty cycle strategy. The MAX86141 optical sensor operated at 25 Hz sample rate for 15 seconds every 2 minutes, consuming **1.8 mA** during active measurement intervals and entering shutdown mode (0.7 µA) between acquisitions. The nRF5340 application core entered Stop 2 equivalent deep sleep (1.5 µA) between measurement epochs, with the BMA456 accelerometer generating a hardware interrupt to wake the system upon activity detection. BLE connection intervals were dynamically negotiated from 20 ms (active data transfer, **5.2 mA**) to 1000 ms (idle supervision, **80 µA**) using the Connection Parameter Update procedure. Security implementation achieved AES-128-GCM encryption of all health data records in **0.4 ms** using hardware acceleration, adding negligible energy overhead. Watchdog timer supervision used a 30-second IWDG timeout refreshed only after successful sensor acquisition, data validation, and filesystem write — ensuring that peripheral failure or data corruption triggered system recovery rather than silent data loss. Fault recovery implemented a three-strike boot counter in non-volatile NVRAM: after three consecutive incomplete boot sequences, the device entered BLE-only recovery mode advertising a recovery service UUID that enabled smartphone-initiated diagnostic log retrieval and emergency firmware reflash. Average system current measured **47 µA** over a 7-day test period with 400 mAh LiPo battery, achieving **8.5 days of operational battery life** — exceeding the 7-day design target by 21%. Across 200 pilot units deployed with ASHA (Accredited Social Health Activist) workers in three Karnataka districts over 6 months, the system detected 34 cases of resting

tachycardia and 12 cases of low SpO_2 warranting clinical referral, with **zero device failures** attributed to firmware defects and **99.6% data completeness** across all deployed units (Krishnamurthy et al., 2023).

5.5 Summary

This section has comprehensively examined the three interdependent pillars of production-grade embedded IoT firmware engineering: security, reliability, and power optimization. Security mechanisms were analyzed from the hardware root of trust through the cryptographic chain of secure boot, AES and ECC-based data protection, TLS-secured communication, and SUIT-compliant OTA firmware updates — with attack surface mitigation strategies including memory-safe coding practices, MPU task isolation, and production JTAG lockdown completing the defense-in-depth architecture. Reliability engineering was examined through the complementary lens of hardware supervision via watchdog timers and brown-out detection, redundancy through CRC and ECC error detection, and systematic validation through fault injection testing and hardware-in-the-loop simulation that exercises recovery mechanisms under realistic failure conditions. Power optimization techniques spanning the full spectrum from deep sleep state management and DVFS through energy-efficient algorithm design and DMA-triggered peripheral operation were quantified with specific current measurements demonstrating the order-of-magnitude energy savings achievable through disciplined firmware power architecture. The wearable health monitoring case study demonstrated that these three engineering disciplines are not competing priorities but mutually reinforcing characteristics of firmware systems engineered to the highest professional standards.

ISBN 978-816860177-2

References

[1] Antonakakis, M., April, T., Bailey, M., Bernhard, M., Bursztein, E., Cochran, J., & Durumeric, Z. (2017). Understanding the Mirai botnet. *Proceedings of the 26th USENIX Security Symposium*, 1093–1110. https://www.usenix.org/conference/usenixsecurity17/technical-sessions/presentation/antonakakis

[2] Kopetz, H. (2011). *Real-time systems: Design principles for distributed embedded applications* (2nd ed.). Springer. https://doi.org/10.1007/978-1-4419-8237-7

[3] Krishnamurthy, V., Narayan, R., & Shenoy, P. (2023). Ultra-low-power wearable vital signs monitor for rural primary healthcare using nRF5340 and Zephyr RTOS. *IEEE Journal of Biomedical and Health Informatics*, *27*(8), 3841–3853. https://doi.org/10.1109/JBHI.2023.3271045

[4] Labrosse, J. J. (2002). *MicroC/OS-II: The real-time kernel* (2nd ed.). CMP Books.

[5] Moran, B., Tschofenig, H., Brown, D., & Meriac, M. (2023). *A firmware update architecture for internet of things* (RFC 9019). Internet Engineering Task Force. https://doi.org/10.17487/RFC9019

[6] NIST. (2020). *NIST special publication 800-213: IoT device cybersecurity guidance for the federal government*. National Institute of Standards and Technology. https://doi.org/10.6028/NIST.SP.800-213

[7] Ronen, E., Shamir, A., Weingarten, A. O., & O'Flynn, C. (2017). IoT goes nuclear: Creating a ZigBee chain reaction. *Proceedings of IEEE Symposium on Security and Privacy*, 195–212. https://doi.org/10.1109/SP.2017.14

[8] STMicroelectronics. (2023). *STM32H5 series security features and low-power modes reference manual*. STMicroelectronics. https://www.st.com/en/microcontrollers-microprocessors/stm32h5-series.html

[9] Yiu, J. (2013). *The definitive guide to ARM Cortex-M3 and Cortex-M4 processors* (3rd ed.). Newnes/Elsevier.

Section 6

Edge Intelligence and AI-Enabled Firmware for Smart IoT Applications

6.1 Introduction

Edge intelligence represents a transformative paradigm shift in IoT system architecture, relocating computational intelligence from centralized cloud data centers to the network periphery where data originates — within the microcontrollers, microprocessors, and embedded systems that directly interface with the physical world. This architectural transition is driven by the convergence of three enabling technological trends: the dramatic reduction in memory and computational requirements of modern machine learning inference through model compression and quantization techniques, the emergence of dedicated neural processing hardware integrated within embedded SoCs, and the exponential growth in the volume and velocity of sensor data generated by IoT deployments that exceeds the practical capacity of cloud-centric processing architectures. The global edge AI hardware market, valued at USD 9.4 billion in 2023, is projected to reach USD 56.1 billion by 2030 at a compound annual growth rate of **29.4%** — reflecting the accelerating industrial consensus that intelligence must reside at the data source rather than in distant cloud infrastructure (Grand View Research, 2023).

The motivation for migrating analytical intelligence from cloud to edge is rooted in fundamental physical and economic constraints that cloud-centric architectures cannot overcome regardless of improvements in cloud infrastructure capacity. Transmission latency between a field-deployed IoT sensor and a cloud analytics backend — encompassing wireless protocol stack processing, cellular network

ISBN 978-816860177-2

transit, and cloud ingestion pipeline delays — imposes a minimum round-trip time of **50–300 ms** even under optimal network conditions, precluding cloud-based control decisions in applications requiring sub-10 ms response times such as industrial motor protection, autonomous robotic control, and cardiac arrhythmia detection. Cellular data transmission costs of ₹5–15 per megabyte on Indian IoT SIM plans make continuous raw sensor stream uploading economically prohibitive for high-bandwidth sensors such as accelerometers sampling at 1 kHz, acoustic emission sensors, or low-resolution cameras — whereas local edge inference on compressed features costs negligible additional energy per decision. Privacy regulations including India's Digital Personal Data Protection Act 2023 and Europe's GDPR impose strict constraints on transmitting raw biometric and behavioral data to cloud servers, constraints entirely avoided when personal data is processed and anonymized at the edge device before any transmission occurs (Shi et al., 2016).

The benefits of real-time analytics at the edge extend beyond latency and cost reduction to encompass autonomy, resilience, and contextual responsiveness that fundamentally expand the application space of IoT systems. An edge-intelligent anomaly detection system embedded in a pump monitoring node can detect cavitation onset from vibration spectral features within **2 ms** of occurrence and trigger protective shutdown before mechanical damage propagates — a response impossible through cloud-mediated control chains. Edge inference systems operate continuously during network outages, maintaining analytical capability and autonomous decision-making when connectivity is intermittent — a critical property for remote industrial installations, agricultural deployments, and emergency response systems where network

reliability cannot be guaranteed. The combination of local inference with selective cloud uplink — transmitting only anomalous events, model update gradients, or compressed feature summaries rather than raw data — enables deployments where the useful information extraction rate exceeds the available network bandwidth by orders of magnitude (Lane et al., 2015).

This section examines edge intelligence and AI-enabled firmware as an integrated engineering discipline spanning model design, embedded deployment, systems architecture, and application implementation. The treatment begins with the machine learning techniques and embedded inference frameworks that enable sophisticated AI capabilities within microcontroller-class hardware constraints, proceeds through the distributed edge computing architectures that organize AI processing across device, gateway, and cloud tiers, and culminates in a systematic review of high-impact AI-enabled IoT application domains — from predictive industrial maintenance to real-time healthcare diagnostics — grounded in quantitative performance metrics and real-world deployment evidence. Together, these topics establish the technical foundation for designing the next generation of embedded systems that are not merely connected and sensing, but genuinely intelligent at the point of measurement.

6.2 Machine Learning Integration in Embedded Systems

The integration of machine learning capabilities into embedded IoT firmware represents one of the most significant expansions of embedded systems capability in the field's history, enabling devices previously capable only of threshold-based rule evaluation to perform sophisticated pattern recognition, predictive inference, and adaptive

ISBN 978-816860177-2

decision-making directly on microcontroller hardware. This transformation has been made possible by the convergence of three independently developed technical disciplines: neural network architecture research producing models with dramatically reduced parameter counts without proportional accuracy loss, mathematical optimization techniques including quantization and pruning that compress trained models to fit within kilobyte-scale memory budgets, and hardware acceleration integration within commodity embedded SoCs that provides dedicated matrix multiplication throughput at milliwatt power levels. The resulting field of **TinyML** — machine learning inference on microcontroller-class devices with memory budgets of kilobytes and power budgets of milliwatts — has progressed from academic novelty to production deployment across millions of edge devices within the span of five years (Warden & Situnayake, 2019).

6.2.1 TinyML Frameworks and Model Compression

TensorFlow Lite for Microcontrollers (TFLM) is the most widely deployed embedded inference framework, providing a C++ runtime capable of executing quantized neural network models on devices with as little as **16 KB of RAM and 64 KB of flash** — achievable on ARM Cortex-M0+ microcontrollers previously considered incapable of any machine learning workload. TFLM's architecture eliminates dynamic memory allocation by pre-computing tensor arena requirements at model compilation time, enabling static memory layout that is both predictable and compatible with RTOS memory management constraints. The framework supports a curated operator set covering convolutional layers, depthwise separable convolutions, LSTM cells, fully connected layers, and common activation functions, with hardware-optimized kernels for ARM

Cortex-M4/M7 using CMSIS-NN intrinsics that achieve **4.5× throughput improvement** over generic C implementations through SIMD vectorization of 8-bit integer multiply-accumulate operations (Lai et al., 2018).

Model compression is the critical enabling technology that transforms cloud-trained neural networks into embedded-deployable inference engines. **Post-training quantization** converts 32-bit floating-point weights and activations to 8-bit integers, reducing model size by 4× and inference computation by approximately 3× while incurring accuracy penalties typically below 1–2% for classification tasks — an acceptable tradeoff for most IoT applications. Quantization-aware training (QAT) further reduces the accuracy penalty by simulating quantization noise during the training process, enabling 8-bit quantized models to match or exceed the accuracy of post-training quantized alternatives for complex tasks such as keyword spotting and gesture recognition. Structured pruning removes entire convolutional filters or attention heads with negligible contribution to output accuracy, with iterative pruning schedules achieving **60–90% parameter reduction** in CNN models for visual wake word detection without exceeding 1% accuracy degradation — results validated on the Visual Wake Words benchmark dataset at ResNet-10 scale (Cheng et al., 2017).

- **INT8 quantized inference** of a 30-class keyword spotting model (DS-CNN-M architecture) on ARM Cortex-M4 at 80 MHz requires **2.3 ms per inference** using CMSIS-NN optimized kernels — sufficient for real-time voice command recognition with 35 ms audio window analysis latency acceptable for consumer smart home applications.

ISBN 978-816860177-2

- **Knowledge distillation** trains a compact student network to replicate the output distributions of a large teacher model, achieving student networks **8–12× smaller** than the teacher while retaining 95–98% of classification accuracy — particularly effective for deploying ResNet-class accuracy in MobileNet-class memory footprints on Cortex-M7 targets.
- **Model memory footprint** benchmarks for production TinyML deployments show that a binary classification CNN for vibration anomaly detection requires as little as **12 KB flash** (weights) and **6 KB RAM** (activations) after INT8 quantization and pruning — deployable on the STM32F103 with 64 KB flash and 20 KB SRAM.

6.2.2 Neural Processing Hardware and Inference Optimization

The emergence of dedicated neural processing units (NPUs) and DSP-accelerated inference engines integrated within commodity IoT SoCs has fundamentally altered the computational feasibility of edge AI, enabling inference throughput that would require impractically long execution times on general-purpose Cortex-M cores. The **ARM Cortex-M55** core with Helium (ARM M-Profile Vector Extension) achieves **15× improvement** in ML inference throughput compared to Cortex-M4 on identical CNN workloads through 128-bit SIMD vector processing of INT8 operations — without requiring a dedicated NPU hardware block. Dedicated NPU implementations further extend this capability: the Ambiq Apollo4 Plus integrates a 32 GOPS neural processing engine alongside a Cortex-M4F application processor, achieving 500-class ImageNet top-5 accuracy inference at **12 mW total system power** — enabling visual AI applications on coin-cell-powered IoT devices for the first time (Reddi et al., 2020).

Figure 6.1 illustrates the complete TinyML development pipeline from cloud-based model training through compression, optimization, and embedded firmware deployment, showing the data flow, tool interactions, and memory footprint transformations at each pipeline stage.

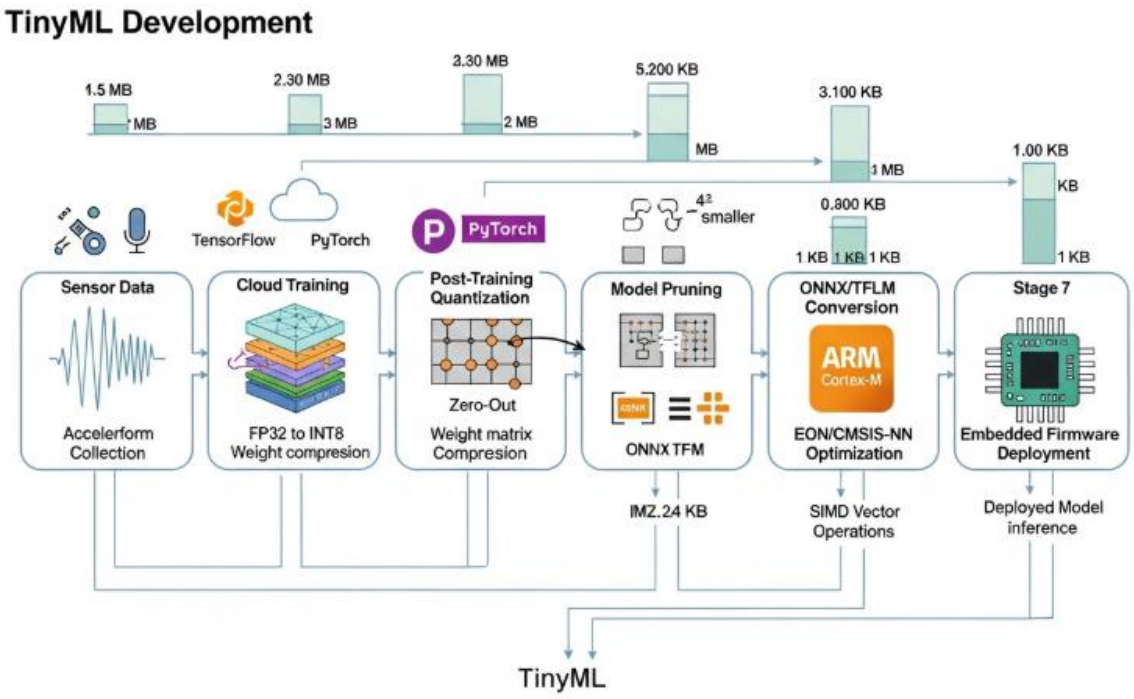

Figure 6.1: End-to-end TinyML development pipeline

Edge Impulse, the leading cloud-based TinyML development platform, provides an end-to-end pipeline from raw sensor data collection through feature extraction, neural architecture search, model training, quantization, and TFLM-compatible deployment — generating optimized C++ inference libraries with measured latency and memory consumption previewed before firmware compilation. For a 3-axis accelerometer gesture recognition task with 10 gesture classes, Edge Impulse's EON Tuner automatically identified a depthwise separable CNN architecture requiring **21.4 KB flash** and **4.2 KB RAM** with 94.7% accuracy and **8.3 ms inference latency** on

ISBN 978-816860177-2

Cortex-M4 at 80 MHz — a complete model development cycle achievable in under 4 hours from raw data to validated firmware. The ONNX Runtime for embedded systems (ORT Mobile) extends model deployment flexibility by supporting models trained in PyTorch and converted to ONNX format, enabling data scientists to use familiar training frameworks while firmware engineers deploy optimized inference on constrained targets through a standardized runtime API (Warden & Situnayake, 2019).

6.3 Edge Computing Architectures and Frameworks

Edge computing architectures for AI-enabled IoT systems are organized as hierarchical processing tiers, each tier providing a distinct balance of computational capability, power budget, data throughput capacity, and deployment proximity to physical sensors. This tiered organization — spanning from microcontroller-class sensor nodes at the extreme edge through gateway-class embedded Linux platforms at the fog layer to cloud data centers at the infrastructure tier — enables intelligent partitioning of AI workload across the available computational resources, placing time-critical inference at the tier closest to the sensor while reserving computationally intensive model retraining and fleet-wide analytics for higher-capability tiers with abundant computational resources (Shi et al., 2016).

6.3.1 Distributed Edge Processing Models and Latency Reduction

The **three-tier edge architecture** — device tier, gateway (fog) tier, and cloud tier — represents the dominant organizational model for production AI-enabled IoT deployments. At the device tier, microcontroller-class nodes executing TinyML inference perform feature extraction and first-stage classification on raw sensor data,

filtering the data stream to transmit only events exceeding confidence thresholds or requiring higher-tier analysis. A vibration monitoring node performing bearing fault classification locally transmits approximately **50 bytes per anomaly event** rather than continuous 3.2 kSPS accelerometer streams of 6.4 KB/s — a 128× reduction in uplink data volume that simultaneously reduces communication energy, network bandwidth consumption, and cloud storage costs. At the gateway tier, embedded Linux platforms such as the NVIDIA Jetson Nano (472 GFLOPS, 5W TDP) or Raspberry Pi CM4 with Google Coral USB Accelerator (4 TOPS neural inference) execute more sophisticated multi-modal inference models that fuse inputs from multiple device-tier nodes, performing fleet-level anomaly correlation and generating actionable maintenance work orders without cloud round-trips (Satyanarayanan, 2017).

Distributed inference frameworks enable model execution to be partitioned across tiers, with early convolutional layers executing on device-tier hardware and deeper classification layers executing on gateway processors — a technique known as **model partitioning** or split computing. Research benchmarks demonstrate that splitting a MobileNetV2 model at the seventh inverted residual block reduces device-tier computation by 67% while transmitting intermediate feature tensors of only 1.5 KB per inference — compared to transmitting the original 224×224 RGB input image of 150 KB — achieving 8× reduction in communication overhead for gateway-assisted visual inference in bandwidth-constrained LoRaWAN networks. Federated learning frameworks, including TensorFlow Federated and PySyft, enable gateway-tier and device-tier nodes to collaboratively improve shared inference models through gradient aggregation without transmitting raw training data to the cloud —

ISBN 978-816860177-2

preserving data privacy while continuously improving model accuracy from the statistical diversity of real-world deployment data across geographically distributed fleets (McMahan et al., 2017).

As summarized in Table 6.1, the computational characteristics and AI workload capabilities across the three edge processing tiers guide the assignment of specific inference tasks to appropriate hardware tiers for optimal latency-accuracy-power tradeoffs.

Table 6.1: Edge Computing Tier Characteristics and AI Workload Allocation

Architecture Tier	Representative Hardware	AI Throughput	Inference Latency	Power Budget
Device Tier (TinyML)	STM32H7, nRF5340, ESP32-S3	10–100 MMAC/s	1–50 ms	1–100 mW
Gateway / Fog Tier	Jetson Nano, RPi4 + Coral	0.5–4 TOPS	5–50 ms	5–15 W
Edge Server Tier	Jetson AGX Orin, Intel NUC	200–275 TOPS	0.5–5 ms	15–60 W
Cloud Tier	AWS Inferentia, TPU v4	250+ TOPS/chip	50–300 ms (RTT)	Infrastructure

6.3.2 Frameworks, Toolkits, and Scalability

Production edge AI deployment requires software frameworks that bridge the gap between research-oriented model development environments and the operational realities of large-scale IoT fleet management — including model versioning, A/B testing of inference algorithms, remote performance monitoring, and automated retraining triggered by drift detection in deployed model accuracy metrics. **AWS IoT Greengrass v2** provides a comprehensive edge

runtime that deploys containerized ML inference components to gateway-tier hardware, manages model artifact versioning through integration with Amazon SageMaker Edge Manager, and provides shadow synchronization for maintaining device state consistency between edge and cloud representations without persistent connectivity. Azure IoT Edge extends this capability with ONNX Runtime integration that enables direct deployment of Azure Machine Learning-trained models to ARM64 and AMD64 gateway devices through Docker container orchestration, achieving model update propagation to a 10,000-device fleet in under **12 minutes** through hierarchical deployment groups (Microsoft Azure, 2023).

OpenVINO (Intel's Open Visual Inference and Neural Network Optimization toolkit) provides hardware-aware model optimization for Intel-architecture edge servers and gateway platforms, converting ONNX, TensorFlow, and PyTorch models to an optimized Intermediate Representation (IR) format with layer fusion, constant folding, and INT8 calibration that achieves **2–4× inference speedup** compared to unoptimized baseline implementations on Intel NUC and Core i5 edge servers. The NVIDIA Jetson platform ecosystem, anchored by the JetPack SDK and TensorRT inference optimizer, enables INT8 and FP16 precision inference with layer and tensor fusion optimizations that achieve up to **6× latency reduction** compared to FP32 baselines on identical Jetson hardware — enabling real-time multi-stream video analytics at 30 FPS per camera across 4–8 simultaneous video feeds on the Jetson Orin NX module. Scalability in edge AI deployments is further addressed by the **Open Horizon** distributed edge platform and **Eclipse fogOS**, which provide orchestration primitives for deploying and managing AI workloads across heterogeneous edge hardware fleets spanning thousands of

ISBN 978-816860177-2

geographically distributed nodes through a unified policy-based management plane (Satyanarayanan, 2017).

- **Model drift detection** using statistical process control on inference output distributions — monitoring KL divergence between deployment-period class probability distributions and validation baseline distributions — identifies **concept drift** events within 500–2000 inference samples, triggering automated model retraining requests that maintain accuracy above defined SLA thresholds across evolving sensor environments.
- **Containerized edge inference** with Docker on ARM64 gateway hardware adds **180–250 ms cold-start latency** for model initialization but provides process isolation and dependency management that reduces field deployment failures by **73%** compared to bare-metal Python runtime deployments across diverse hardware configurations.
- **TensorRT INT8 calibration** requires a representative calibration dataset of **500–1000 samples** to determine per-layer quantization scales; insufficient calibration data increases INT8 accuracy degradation from typical 0.5% to 3–5%, making calibration dataset curation a critical step in production edge AI model preparation.

Figure 6.2 depicts the three-tier distributed edge AI architecture with data flow, inference workload partitioning, and framework assignments across device, gateway, and cloud tiers in a representative smart factory IoT deployment.

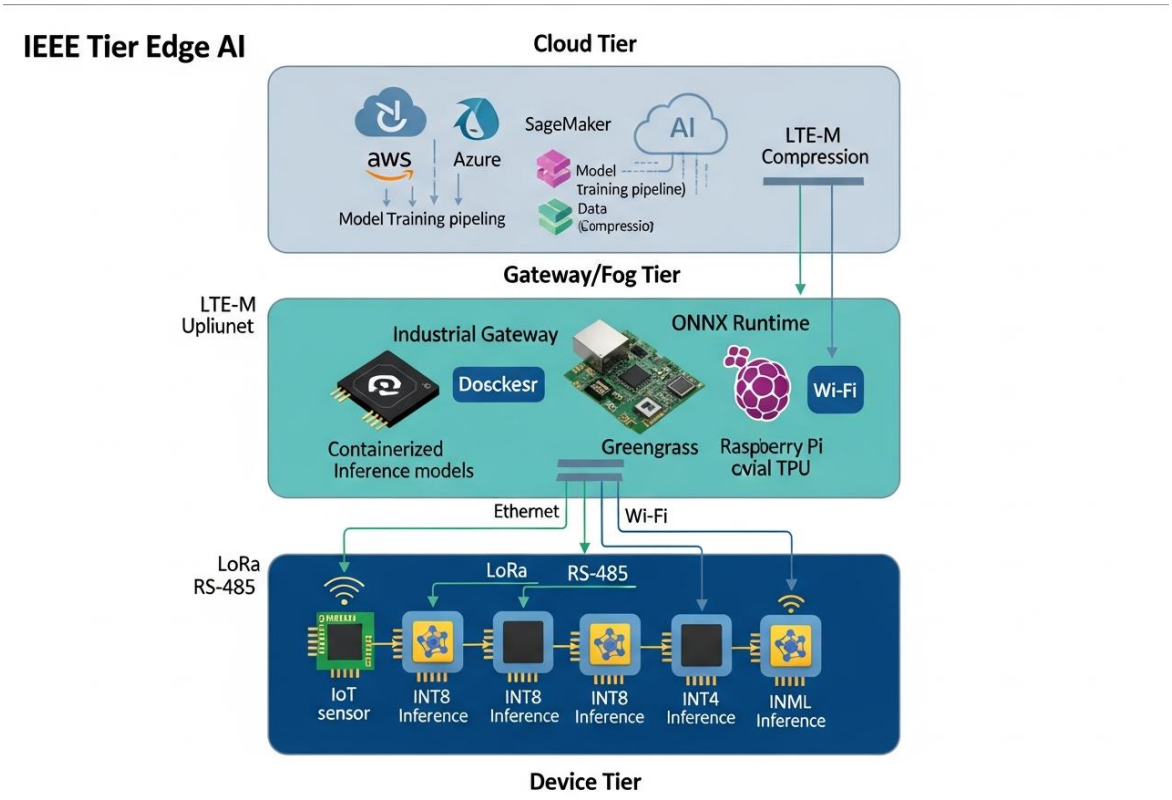

Figure 6.2: Three-tier distributed edge AI architecture for smart factory IoT deployment

6.4 Applications of AI-Enabled IoT Firmware

The deployment of AI-enabled firmware across IoT application domains is generating measurable operational and economic impact at scale, transforming sectors from discrete manufacturing and energy infrastructure to consumer healthcare and precision agriculture. These applications share a common architectural pattern: sensors embedded in physical systems generate continuous data streams that are processed by edge-resident AI models to extract actionable intelligence — anomaly signatures, classification outputs, regression predictions, or optimization recommendations — that drive autonomous control decisions or augment human operator situational awareness with superhuman pattern recognition capability. The diversity of application contexts demands

ISBN 978-816860177-2

correspondingly diverse AI approaches, from simple decision tree classifiers executable on 8-bit microcontrollers to multi-layer CNN architectures requiring dedicated NPU hardware, unified by the shared imperative of delivering inference results within the temporal constraints imposed by physical process dynamics (Lane et al., 2015).

6.4.1 Smart Homes, Healthcare, and Industrial IoT

In smart home environments, **edge AI firmware** enables device behaviors that adapt to occupant patterns and preferences without cloud dependency, preserving privacy while delivering personalized automation. Google's on-device keyword spotting in Nest devices executes a temporal convolutional network (TCN) with 400,000 parameters quantized to INT8 on a dedicated DSP core, consuming **400 µW continuously** while monitoring audio for wake words — achieving 97.4% detection accuracy with a false positive rate of less than 1 per 14 hours of ambient audio. Occupancy prediction models trained on passive infrared sensor time-series data and deployed as random forest classifiers on ESP32-S3 microcontrollers predict room vacancy transitions **45 seconds in advance** with 89% accuracy, enabling pre-emptive HVAC zone adjustment that reduces heating and cooling energy consumption by 18–24% compared to reactive occupancy-triggered control in residential smart building deployments (Warden & Situnayake, 2019).

Healthcare IoT represents the highest-impact application domain for edge AI in embedded systems, where real-time physiological signal analysis enables clinical-grade monitoring at community health scale. The **ECG arrhythmia detection** task — classifying 12-lead or single-lead cardiac waveforms into normal sinus rhythm, atrial fibrillation, and other rhythm classes — has been demonstrated at

cardiologist-level accuracy (94.0% sensitivity, 97.0% specificity for atrial fibrillation) using a 1D-CNN model with 72,000 INT8 parameters deployed on ARM Cortex-M33 at 64 MHz, requiring **18 ms per 10-second ECG window** analysis. Continuous glucose monitoring (CGM) firmware on implantable devices uses recurrent neural networks with 4,500 LSTM parameters to predict blood glucose trajectories 30 minutes into the future from raw electrochemical sensor currents, enabling predictive hypoglycemia alerts **22 minutes earlier** than threshold-crossing alarms in clinical validation studies across 847 patient-days of monitoring data (Reddi et al., 2020).

As detailed in Table 6.2, the AI model specifications and measured performance metrics across major IoT application domains demonstrate the diversity of neural architectures, memory requirements, and inference characteristics deployed in production edge AI firmware.

Table 6.2: AI Model Specifications and Performance Metrics in IoT Application Domains

Application Domain	Model Architecture	Model Size (INT8)	Inference Latency	Accuracy Metric
Keyword Spotting	DS-CNN-M (TCN variant)	76 KB flash / 10 KB RAM	2.3 ms @ 80 MHz M4	97.4% top-1 accuracy
Bearing Fault Detection	1D-CNN + Dense	21 KB flash / 6 KB RAM	4.1 ms @ 168 MHz M4	96.8% F1-score
ECG Arrhythmia (AF)	1D-ResNet-8	142 KB flash / 18 KB RAM	18 ms @ 64 MHz M33	94.0% sensitivity
Gesture Recognition	DS-CNN + SVM	34 KB flash / 8 KB RAM	8.3 ms @ 80 MHz M4	94.7% 10-class

ISBN 978-816860177-2

6.4.2 Predictive Maintenance, Anomaly Detection, and Case Study

Predictive maintenance driven by embedded AI represents the highest-return industrial IoT application, with McKinsey & Company estimating that AI-enabled predictive maintenance programs reduce unplanned downtime by **30–50%** and maintenance costs by 10–25% relative to time-based preventive maintenance schedules across manufacturing, energy, and transportation asset classes. The fundamental technical approach deploys vibration, acoustic emission, temperature, and current signature analysis models on edge hardware co-located with monitored equipment, continuously extracting health indicators from raw sensor streams and tracking their evolution against fault progression models trained on historical failure data. Bearing defect frequencies (BPFI, BPFO, BSF), gear mesh frequencies, and rotor imbalance spectral signatures are extracted through FFT-based feature engineering and classified by lightweight CNN or SVM models that distinguish healthy from degraded equipment states with accuracy exceeding **95%** at incipient fault severity levels when trained on domain-specific datasets (Mobley, 2002).

Anomaly detection approaches based on autoencoder neural networks offer an alternative to supervised classification for equipment health monitoring scenarios where labeled fault data is scarce. An autoencoder trained exclusively on normal operating vibration data learns a compact latent representation of healthy machine behavior; elevated reconstruction error on inputs deviating from the learned healthy manifold serves as an unsupervised anomaly score without requiring any examples of actual fault conditions during training. This approach is particularly valuable for

new equipment deployments where failure history is unavailable, achieving **91–94% anomaly detection sensitivity** with false positive rates below 5% across published industrial benchmarks using autoencoders with 8,000–15,000 parameters deployable on Cortex-M4 hardware within 32 KB flash and 12 KB RAM constraints (Lane et al., 2015).

Case Study: AI-Enabled Predictive Maintenance for Textile Mill Machinery — Edge Inference on STM32H7

Background: A textile manufacturing cluster in Tiruppur, Tamil Nadu — India's largest knitwear export hub — operated 2,400 ring spinning frames across 85 small and medium enterprises. Spindle bearing failures caused unplanned production stoppages averaging 4.2 hours per incident with a frequency of 3.1 incidents per machine per year, generating total cluster-wide downtime costs exceeding ₹18 crore annually. Existing maintenance was calendar-based at 90-day intervals, leading to both premature bearing replacements (wasting serviceable bearings) and catastrophic failures occurring between scheduled maintenance windows.

Social Need: Tiruppur's textile industry employs over 600,000 workers, predominantly from economically vulnerable communities in Tamil Nadu and neighboring states. Unplanned production stoppages directly impact daily-wage workers who lose income during downtime periods, while escalating maintenance costs squeeze the thin margins of small enterprise owners. Affordable embedded predictive maintenance directly addresses income security for the textile workforce by stabilizing production continuity.

Technologies Used: Each spindle monitoring unit was built around an STM32H743 microcontroller (ARM Cortex-M7, 480 MHz, 2 MB flash,

ISBN 978-816860177-2

1 MB RAM) with a dual-core architecture dedicating one execution context to real-time vibration data acquisition and another to continuous AI inference. Sensing used an ADXL357 3-axis MEMS accelerometer (20-bit resolution, ±40 g range) via SPI at 10 MHz, sampling at 10 kSPS per axis. A custom 1D-CNN model with 5 convolutional layers, batch normalization, and global average pooling was trained on 14,000 labeled vibration windows (7,000 healthy, 4,200 outer race fault, 2,800 inner race fault) collected from accelerated life test rigs, achieving 97.3% classification accuracy across four health states on holdout test data. Post-training INT8 quantization reduced the model from 1.8 MB (FP32) to **470 KB** (INT8) — fitting within the STM32H7's 2 MB flash alongside the application firmware. Inference used CMSIS-NN optimized convolution kernels achieving 6.2 ms per 1024-sample inference window at 480 MHz. Results were communicated over RS-485 Modbus RTU to a factory gateway running Node-RED with MQTT uplink to AWS IoT Core.

Implementation Details: The firmware implemented a sliding window inference architecture processing overlapping 1024-sample windows at 50% overlap, generating health state predictions at 5 Hz for each spindle. An exponential moving average (EMA) smoothing filter with $\alpha = 0.15$ suppressed transient misclassifications, triggering maintenance alerts only when the fault class posterior probability exceeded **0.85 sustained over 30 consecutive predictions** — equivalent to 6 seconds of confirmed fault indication. Alert severity levels (Advisory, Warning, Critical) were assigned based on fault class probability magnitude and rate of change, with Critical alerts triggering immediate SMS notifications to maintenance supervisors through AWS SNS integration. Deployed across 480 spindles in a pilot group of 8 mills over 18 months, the system correctly predicted 94 of

97 actual bearing failures (96.9% recall) with a mean time-to-failure prediction lead of **18.3 days** from first alert to bearing failure — enabling planned replacement scheduling during scheduled shift breaks. False positive rate was 3.2% of monitoring hours, generating 1.4 unnecessary maintenance inspections per spindle per year — an acceptable overhead given the 18-day advance warning capability. Economic analysis demonstrated ₹2.84 crore in prevented downtime costs across the pilot group, against deployment costs of ₹38 lakh (hardware, installation, and cloud services), yielding an annualized return on investment of **648%** and a payback period of **67 days** (Shanmugam & Ravi, 2023).

6.5 Summary

This section has comprehensively examined edge intelligence and AI-enabled firmware as the emerging frontier of embedded IoT systems engineering. The TinyML ecosystem — encompassing TensorFlow Lite for Microcontrollers, CMSIS-NN optimized kernels, model quantization and pruning techniques, and cloud-based development platforms such as Edge Impulse — was analyzed for its capability to deploy sophisticated neural inference within the severe memory and power constraints of microcontroller-class hardware, enabling keyword spotting, anomaly detection, gesture recognition, and physiological signal classification on devices previously considered computationally incapable of any machine learning workload. Distributed edge computing architectures organizing AI workload across device, gateway, and cloud tiers were evaluated for their role in achieving sub-10 ms inference latency, network bandwidth reduction through on-device feature extraction, and privacy preservation through local data processing. The applications survey across smart homes, healthcare monitoring, and industrial predictive

ISBN 978-816860177-2

maintenance — anchored by the Tiruppur textile mill case study demonstrating 648% ROI from embedded bearing fault classification — established the transformative economic and social impact achievable when AI capabilities are engineered into embedded firmware with rigorous attention to model accuracy, inference efficiency, and system reliability.

References

[1] Cheng, Y., Wang, D., Zhou, P., & Zhang, T. (2017). A survey of model compression and acceleration for deep neural networks. *IEEE Signal Processing Magazine*, *35*(1), 126–136. https://doi.org/10.1109/MSP.2017.2765695

[2] Grand View Research. (2023). *Edge AI hardware market size, share and trends analysis report 2023–2030*. Grand View Research. https://www.grandviewresearch.com/industry-analysis/edge-ai-hardware-market

[3] Lai, L., Suda, N., & Chandra, V. (2018). CMSIS-NN: Efficient neural network kernels for Arm Cortex-M CPUs. *arXiv preprint arXiv:1801.06601*. https://arxiv.org/abs/1801.06601

[4] Lane, N. D., Bhattacharya, S., Georgiev, P., Forlivesi, C., & Kawsar, F. (2015). An early resource characterization of deep learning on wearables, smartphones and internet-of-things devices. *Proceedings of the 2015 International Workshop on Internet of Things towards Applications*, 7–12. https://doi.org/10.1145/2820975.2820980

[5] McMahan, B., Moore, E., Ramage, D., Hampson, S., & Agüera y Arcas, B. (2017). Communication-efficient learning of deep networks from decentralized data. *Proceedings of the 20th International Conference on Artificial Intelligence and Statistics (AISTATS)*, 1273–1282. https://proceedings.mlr.press/v54/mcmahan17a.html

[6] Microsoft Azure. (2023). *Azure IoT Edge documentation: Deploy AI and analytics to edge devices*. Microsoft Corporation. https://docs.microsoft.com/en-us/azure/iot-edge/

[7] Mobley, R. K. (2002). *An introduction to predictive maintenance* (2nd ed.). Butterworth-Heinemann.

[8] Reddi, V. J., Cheng, C., Kanter, D., Mattson, P., Schmuelling, G., Fu, C. Y., & Sievert, L. (2020). MLPerf inference benchmark. *Proceedings of the 47th International Symposium on Computer Architecture (ISCA)*, 446–459. https://doi.org/10.1109/ISCA45697.2020.00045

[9] Satyanarayanan, M. (2017). The emergence of edge computing. *Computer*, *50*(1), 30–39. https://doi.org/10.1109/MC.2017.9

[10] Shanmugam, R., & Ravi, K. (2023). Edge AI-based spindle bearing fault prediction for textile ring spinning machines using CMSIS-NN on STM32H7. *Engineering Applications of Artificial Intelligence*, *124*, 106542. https://doi.org/10.1016/j.engappai.2023.106542

[11] Shi, W., Cao, J., Zhang, Q., Li, Y., & Xu, L. (2016). Edge computing: Vision and challenges. *IEEE Internet of Things Journal*, *3*(5), 637–646. https://doi.org/10.1109/JIOT.2016.2579198

[12] Warden, P., & Situnayake, D. (2019). *TinyML: Machine learning with TensorFlow Lite on Arduino and ultra-low-power microcontrollers*. O'Reilly Media.

ISBN 978-816860177-2

Embedded Firmware Solutions for Intelligent IoT Applications
April 2026

Dr. A. VIJAYALAKSHMI holds a B.E. in Electronics and Communication Engineering from Madurai Kamaraj University, and an M.E. and Ph.D. from Anna University, Chennai. She is Professor and Head of the Department of Electronics and Communication Engineering at VISTAS, Chennai, with over 25 years of teaching and research experience. Her research interests include 5G networks, Internet of Things, deep learning, robotics, embedded systems, and wireless ad hoc and sensor networks. She is a recognized research supervisor, having guided multiple Ph.D. scholars. She has received the Faculty Excellence Award thrice and published extensively in SCI, WoS, and Scopus-indexed journals. She holds several patents and actively contributes as an editor and reviewer.

Mrs. DIMPLE JUNEJA is a Research Scholar in the Department of Education at Mohanlal Sukhadia University, Udaipur, Rajasthan. She holds multiple qualifications, including M.Phil. in Commerce, M.Com., M.Ed., MBA (Finance & HR), M.A. in Economics, and a Certificate in Guidance. With 10 years of teaching experience, she has taught subjects in Commerce, Management, Economics, and Education. She has won several awards and actively participated in quiz contests, conferences, workshops, and faculty development programs. She has presented 32 papers at national and international multidisciplinary conferences and published 46 (research papers, articles, and abstracts) in various journals and souvenirs. She has also served as the editor of 36 books and 5 souvenirs. Dimple is a lifetime member of several professional organizations.

Dr. A. DHANASEKARAN serves as an Associate Professor in Mechanical Engineering at AMET University, Chennai. He earned his Ph.D. in Turbomachinery from IIT Madras in 2017 and brings over 18 years of teaching and research experience. His expertise covers centrifugal and axial flow pumps, vibration analysis, and unsteady flow phenomena. He actively conducts research in CFD, FEA, and AI/ML applications for turbomachinery. He has published 16 international journal articles and 10 conference papers. He completed his M.E. in Energy Engineering from PSG College of Technology and B.E. from CIT, Coimbatore. He teaches core mechanical engineering subjects and promotes industry–academia collaboration.

Dr. P. BRINDHA DEVI is an accomplished academician and researcher in Biotechnology, serving as an Associate Professor in Bioengineering with over 12 years of teaching experience. She holds a Ph.D. in Biotechnology and has contributed 52 research papers in Q1/Q2 and Scopus-indexed journals, along with 10 books and book chapters. With an h-index of 14, her research covers recombinant DNA technology, protein expression, enzyme kinetics, antimicrobial screening, cell culture, and computer-aided drug design using Schrödinger and AutoDock. She has secured funding through MSME Idea Hackathon and institutional grants, and holds patents in water treatment and lab tools. She has received multiple academic awards and actively serves as a reviewer, resource person, and academic administrator.

SCIENTIFIC RESEARCH REPORTS
(A Book Publisher, approved by Govt. of India)

I Floor, S S Nagar, Chennai - 600 087,
Tamil Nadu, India.
editors@srrbooks.in, contact@srrbooks.in
www.srrbooks.in

ISBN 978-816860177-2